HESPERIA

The Journal of the American School of Classical Studies at Athens

Volume 81
2012

HESPERIA

THE JOURNAL OF THE AMERICAN SCHOOL OF CLASSICAL STUDIES AT ATHENS

VOLUME 87 · NUMBER 1
JANUARY–MARCH 2018

American School of Classical Studies at Athens
1827

HESPERIA

Hesperia is published quarterly by the American School of Classical Studies at Athens. Founded in 1932 to publish the work of the American School, the journal now welcomes submissions from all scholars working in the fields of Greek archaeology, art, epigraphy, history, materials science, ethnography, and literature, from earliest prehistoric times onward. *Hesperia* is a refereed journal, indexed in *Abstracts in Anthropology, L'Année philologique, Art Index, Arts and Humanities Citation Index, Avery Index to Architectural Periodicals, Current Contents, IBZ: Internationale Bibliographie der geistes- und sozialwissenschaftlichen Zeitschriftenliteratur, Numismatic Literature, Periodicals Contents Index, Russian Academy of Sciences Bibliographies,* and *TOCS-IN*. The journal is also a member of CrossRef.

The American School of Classical Studies at Athens is a research and teaching institution dedicated to the advanced study of the archaeology, art, history, philosophy, language, and literature of Greece and the Greek world. Established in 1881 by a consortium of nine American universities, the School now serves graduate students and scholars from more than 180 affiliated colleges and universities, acting as a base for research and study in Greece. As part of its mission, the School directs ongoing excavations in the Athenian Agora and at Corinth and sponsors all other American-led excavations and surveys on Greek soil. It is the official link between American archaeologists and classicists and the Archaeological Service of the Greek Ministry of Culture and, as such, is dedicated to the wise management of cultural resources and to the dissemination of knowledge of the classical world. Inquiries about programs or membership in the School should be sent to the American School of Classical Studies at Athens, 6–8 Charlton Street, Princeton, New Jersey 08540-5232.

HESPERIA 81 (2012)
Pages 383–432

GEOPHYSICAL SURVEY AS AN AID TO EXCAVATION AT MITROU

A Preliminary Report

ABSTRACT

Various geophysical methods were used to explore the subsurface of the prehistoric site of Mitrou. Geophysical research was essential for selecting significant areas for excavation as well as for guiding archaeological fieldwork and complementing its results. Resistivity mapping and differential magnetometry detected patterns of well-structured anomalies, suggesting that a regularly laid-out urban complex covered most of the site; electrical resistivity tomographies yielded three-dimensional views of buried structures and indicated promising areas for further exploration. Subsequent excavation uncovered the targeted parts of this complex. The results of this combined research provide new information about crucial periods of change in Greek prehistory.

INTRODUCTION

Geophysical surveys of archaeological sites are an invaluable tool for planning excavations because they enable researchers to focus limited resources on areas where excavation is likely to be fruitful. The authors of this article discuss the surveys that were carried out at the prehistoric site of Mitrou in 2003 and 2005 in order to guide and inform the 2004–2008 excavations.[1] We present an interpretation of the geophysical data along with preliminary results of the excavation and surface survey, offering a loose assessment of their correlation. It is our goal to demonstrate the usefulness of carrying out geophysical survey as an integral part of the archaeological research design.

1. The Mitrou Archaeological Project is a joint undertaking of the University of Tennessee and the 14th Ephorate of Prehistoric and Classical Antiquities (ID′ EPKA) at Lamia, conducted under the auspices of the American School of Classical Studies at Athens and the Greek Archaeological Service. Project directors are Aleydis Van de Moortel, University of Tennessee, and Eleni Zahou, archaeologist with ID′ EPKA. A program of excavation and survey was carried out for five years (2004–2008); study seasons began in 2009 and will continue until final publication of the material is completed. The geophysical sections of this article were written by Gregory Tsokas, and the archaeological parts by Aleydis Van de Moortel. Full acknowledgments for funding and support appear at the end of this article.

Figure 1. Map showing the location of Mitrou in the North Euboian Gulf. B. Lis and T. Ross

The Bronze Age and Early Iron Age site of Mitrou is a small tidal islet of 3.6 ha located in the North Euboian Gulf, roughly 100 m off the coast of Tragana in East Lokris, Greece (Figs. 1, 2). The islet is quite flat, rising gently to the north to about 12 m above sea level. Archaeological remains are strewn over the entire surface and continue in the sea to the east and west of the islet, indicating that relative sea level in prehistoric times was at least 3 m lower than at present. The site at that time was probably not an islet but part of the mainland, situated on a low rise overlooking the sea.

The islet of Mitrou is devoid of modern buildings and has never before been the focus of sustained excavation. We wanted to excavate it for several reasons. Mitrou is one of the largest prehistoric settlements of East Lokris, and it is very well preserved, having been free of substantial occupation since ca. 900 B.C.[2] A surface survey of the islet carried out in 1988–1989 by the Cornell Halai and East Lokris Project (CHELP) found evidence for continuous occupation throughout the Bronze Age and into the Early Iron Age (ca. 3000–900 B.C.).[3] Natural scarps created by the sea on the east and west sides of the islet showed that these remains were well stratified. Such a long, uninterrupted occupational sequence is rare in Greek prehistoric sites, and Mitrou promised to be an ideal site for studying important societal changes in this period. In particular, we wanted to focus on the rise of complex society and the ascent of an archaeologically visible elite at the transition from the Middle Helladic (MH) to Late Helladic (LH) periods, and also on the disintegration of Mycenaean state-level society and its reversion to a simpler society in the final Bronze Age and Early Iron Age.

2. For an overview of prehistoric sites found in East Lokris, see Hope Simpson and Dickinson 1979; Fossey 1990; and yearly reports in the *Archaiologikon Deltion,* especially from 1973 onward. A recent overview of Late Bronze Age and Early Iron Age sites in East Lokris is provided by Van de Moortel (2007); see also the survey of Late Bronze Age sites in Kramer-Hajos 2008.

3. Kramer-Hajos and O'Neill 2008.

Figure 2. Balloon image of the islet of Mitrou at the end of the 2008 excavation season. Photo K. Xenikakis

Constraints of time and budget made it imperative that we concentrate our excavation efforts on those land plots that contained the most promising features; we knew that we would not be able to excavate more than a fraction of the 3.6 ha site in the five-year time span allowed by Greek law.[4] The choice of where to start digging was made difficult, however, by the absence of any articulated architectural remains on the surface. Thus we initiated a program of geophysical surveys to locate architectural features hidden below the surface and identify the most opportune locations for excavation. We also anticipated that the results of the geophysical surveys would complement the finds of our excavation, enabling us to put together a more detailed picture of the site's history. Excavation and geophysical

4. Current Greek law allows a maximum of five years of systematic excavations before publication and it requires excavators to finance expropriation of all land plots in which digging takes place. The duration of our excavation seasons was limited to six to eight weeks per year.

survey were supplemented by a fine-grained vacuum surface survey in 2.5 × 2.5 m grid squares, which provided a detailed overview of artifact distribution and microtopography, as well as by detailed architectural drawings and stratigraphic excavations of the sea scarps on the east and west sides of the islet.[5] All these strands of information are being integrated in a GIS map that will facilitate interpretation of the results.

The following report describes in detail the various geophysical survey techniques employed and the results obtained. Each set of geophysical data is compared with the results of excavations conducted from 2004 to 2008. Then follows a preliminary overview of the settlement history of Mitrou in the LH and Protogeometric (PG) periods as reconstructed from the archaeological and geophysical work. We conclude with a brief assessment of the potential and limitations of geophysical work in archaeological inquiry.

Figure 3 ***(opposite)*****. Layout of the geophysical grid superimposed on a 2006 balloon image of Mitrou. Position of the grid with respect to the ground surface is slightly distorted due to the slightly oblique angle of the photograph. Coordinates follow the Hellenic Geodetic Reference System of 1987.** Photo K. Xenikakis; overlay G. N. Tsokas, P. I. Tsourlos, A. Stampolidis, G. Vargemezis

GEOPHYSICAL SURVEYS IN 2003 AND 2005

The distribution of ancient artifacts on the surface of Mitrou, as well as architectural remains visible in the sea scarps, suggested that the whole island was once covered by man-made structures. For this reason, we carried out geophysical surveys over the entire islet (September 2003, June 2005). Figure 3 shows the layout of the geophysical grid of 20 × 20 m squares established on the surface to facilitate subsequent data processing. This arrangement also gave us some flexibility to cope with the irregularities of the shoreline. The corners of each grid square were marked on the ground by wooden pegs. Squares surveyed with resistance mapping (electrical resistivity survey) have numbers preceded by the letter R, whereas those surveyed with magnetic gradiometry have the prefix G. Five squares surveyed by both methods are labeled with the prefix GR (28, 31–34). Those five squares were chosen at the boundary between the two types of geophysical survey in order to treat problems that might arise when attempting to merge the results of the two methods. The grid square between G77 and R15 was not surveyed because it was littered with scrap iron.

Surveying the whole islet with both methods would have been needlessly time-consuming and expensive. Instead we chose for each type of terrain the method that we expected to be most suitable: resistance mapping

5. After five years of fieldwork (2004–2008), we have excavated 2.2% of the site's surface and carried out a fine-grained pick-up survey over almost 25% of the surface. Most of the remaining surface area of Mitrou was surveyed in much larger units by CHELP in 1988–1989 (Kramer-Hajos and O'Neill 2008). We decided not to conduct drillings across the site with a soil auger to determine the depth and date of the archaeological strata for several reasons. First, we suspected that drilling would be difficult because of the high density of stones in the subsurface. Second, the sea scarps with their continuous ca. 45 m long sections through the settlement and sequences of up to 25 strata already give us a consistent, reliable representation of the site's stratigraphy, as well as of the dramatic north–south slope of bedrock in the northern half of the islet. Finally, geophysical surveys gave us a much more complete understanding of the configuration of buried structures than soil augering could have done. Our fear about the difficulties of augering was confirmed when geologists John Foss and Mark Green carried out core drillings during 2007 and 2008 in two deep excavation trenches and on the eastern shore of the islet with a 3¼″ hand-operated auger; they did not penetrate deeper than 0.3 m, 1.2 m, and 1.8 m, respectively, and did not hit bedrock, nor did they bring up diagnostic pottery fragments. The lowest absolute elevation they reached was 1.8 m below sea level, in a drilling carried out at the eastern shore in the northern half of the islet (Green 2011, p. 341).

in the abandoned open fields in the northeast, central, and east-central parts of the site, and magnetic gradiometry in the olive groves that cover the remainder of the islet. Resistance mapping was chosen as the initial prospecting method mainly because we did not know how the clayey sediments on Mitrou would affect the response of subsurface targets to

the magnetic method. The resistance method was deemed more likely to produce measurable anomalies from architectural remains buried in a clayey environment.[6] On the other hand, it is well known that electrochemical activity in tree roots creates resistance anomalies, and thus we preferred to survey the olive groves using the magnetic method, which is insensitive to this phenomenon.[7]

In addition to conventional geophysical surveys, we conducted resistivity tomographies—vertical cross-sections of the subsurface—in well-defined areas to provide two- or three-dimensional images of buried remains. Because of limitations of time and means, resistivity tomographies were performed at a particular location in either two dimensions or three dimensions, but not both. A pair of two-dimensional tomographies was carried out across the length and width of the islet to study its geological and tectonic setting and investigate the depth of the archaeological strata. Series of parallel tomographies were conducted at specific locations where clear and promising outlines of buried ancient structures had been detected by geophysical mapping. Their aim was to determine the depth of the ruins as well as their three-dimensional configuration, thus aiding in the planning of excavations.[8] These parallel tomographies were carried out in two dimensions and mathematically inverted to create three-dimensional images.

RESISTANCE MAPPING

By sampling the earth's resistance to electrical current at a series of fixed intervals, it is possible to construct a map of subterranean areas of high resistivity. Soil, when it is not arid, is a relatively good conductor of electricity because of the water it contains; stone tends to hold far less moisture and is thus a poor conductor, offering high resistance. Consequently, greater resistivity is indicative of the presence of subsurface features such as bedrock or ancient architectural remains. Since the pattern of resistivity represents the horizontal dimensions of buried features, the images obtained by resistivity mapping resemble a view in plan of concealed architecture.

Methodology

The resistance survey was conducted in September 2003, the year before excavations were scheduled to begin. Heavy rains fell shortly before the survey, ensuring that the resistivity readings would show a good contrast between soil and buried stone. The survey method we employed is a standard mode of resistance mapping worldwide.[9] The earth's resistance is measured at the nodes of a grid established on the ground surface—in this case, a 1×1 m grid established within each one of the 20×20 m squares. Two electrodes are used to insert an electrical current into the ground at two different points. Each current electrode is paired with a probe that measures the drop in potential, indicating the resistance. Thus every measurement involves a total of four electrodes arranged on the ground in one of many possible configurations.[10] Aspinall and Lynam's twin probe array and Clark's pole–pole array are the ones most widely used in archaeological

6. Tsokas et al. 2003, pp. 14–17.

7. Linford 2006, pp. 2214–2215.

8. Subsequent resistivity tomography surveys were carried out in 2006 and 2007. These will be published once detailed comparisons between tomographies and archaeological results have been conducted.

9. Linford 2006, p. 2215.

10. Aitken 1974, pp. 270–271; Tsokas, Tsourlos, and Papadopoulos 2008, p. 84.

prospection.[11] In both configurations one pair of electrodes remains on the ground in fixed position, away from the area being surveyed, while the other pair is carried from point to point on the grid. The need to reposition only two electrodes for each reading presents a definite operational advantage over arrays that require all four electrodes to be moved for each new measurement. For our survey we chose Aspinall and Lynam's twin probe array. Our mobile probes were rigidly attached to a beam that was part of a light, compact frame. The measuring instrument was also attached to the frame so that the whole system could be transported from one measuring station to the next.[12] Data stored in the instrument were downloaded to a laptop computer after the completion of each day's work and some initial data processing was completed.

The size of the targets to be identified was relatively small and their burial depth relatively shallow. Thus we spaced both the mobile and stationary electrode pairs 0.5 m apart to increase the resolution of the measurements. At this spacing, the electrical current penetrates to a depth of about 0.75–1.00 m.[13] The resulting image shows all the anomalies that were detected within 0.75–1.00 m of the ground surface. Readings were taken in a zigzag pattern, stepwise at 1 m intervals along traverses spaced 1 m apart. Over the course of four days we took 400 measurements in each 20 × 20 m grid square, for a total of 13,600 measurements in 34 grid squares covering 13,600 m^2. Because of temporal and financial limitations we did not experiment with decreasing the intervals between readings to increase spatial resolution.

Our goal was to use the resistance data to produce maps that could be easily compared with topographic and archaeological plans. The measured resistances can be mapped in a variety of ways ranging from contour maps to grayscale or color images. In the accompanying resistance maps, more highly resistive areas are depicted in darker gray tones.

Generating the maps required two stages of data processing: edge matching and filtering. Edge matching was necessary to homogenize the data from adjacent grid squares because mismatches in the readings were observed. Some were due to weather changes from one day to the next. Other mismatches were created whenever the stationary probes were moved to a new location. For edge matching we calculated the means of two neighboring rows belonging to two adjacent grids. The difference between those means was then subtracted from all the readings of the grid with the higher mean.

Next, we filtered the data to eliminate noise, minimize the effect of geological structures that might interfere with the response from archaeological objects, separate the signals from different sources buried at different depths, and give the resistance anomalies a more "blocky appearance."[14] The median was calculated on a moving window that then was used to substitute the central value in the window. This process smooths all the data and removes outlying values that presumably have purely technical causes (such as contact resistances). The filtered data were visually compared to the original data to check that no useful information had been discarded. Then the final image was magnified by two-dimensional interpolation using cubic spline functions. Finally, dynamic range compression was performed

11. Aspinall and Lynam 1970, p. 69; Clark 1990, pp. 44–48.

12. The instrument used was an RM-15 from Geoscan Research.

13. Clark 1990, p. 44.

14. Scollar, Weidner, and Segeth 1986, p. 624.

with the arctan technique. At the initial data quality control, the plotting parameters were set separately for each 20 × 20 m grid square in order to enhance the image of the subsurface within that particular square.

Edge matching and filtering were first performed immediately after the completion of the resistance survey in 2003. When we used a magnetic gradiometer to survey the wooded parts of the islet in 2005, we reprocessed the 2003 resistance data in order to achieve the maximum possible match between the 2003 and 2005 results.[15]

Results of the Resistivity Survey

The distribution of the subsurface resistance values is presented here in such a way as to resemble a view in plan of the buried architectural remains as if they had been excavated (Fig. 4).[16] The dark features depict areas of greater resistivity, which may reflect the presence of ruins or bedrock. The dark linear anomalies form geometrical patterns, suggesting that they are the result of human activity. Excavation confirmed the results of the geophysical survey: the distribution of resistance anomalies on the map corresponded to stone walls and concentrations of stones revealed in trenches in the northeast and east-central areas of the islet (Figs. 5–10). Moreover, many features detected by resistance mapping were aligned along NNE–SSW and WNW–ESE axes, and excavation has shown that this was indeed the main orientation of the built environment in the Late Bronze Age and Early Iron Age.

Several linear features form rectangular shapes (Fig. 4). This effect is most pronounced in the eastern part of the image, where the alignment of the anomalies suggests an architectural complex; this includes the outline in squares R9 and R11 of what seems to have been an important apsidal or rectilinear structure. Apsidal structures are prominent in Greek prehistory in the Early Helladic (EH) III and MH periods as well as in LH IIIC and the Early Iron Age—periods that include the major social transitions that are the focus of the Mitrou archaeological project. We therefore decided to begin excavations at this structure; the surrounding area became our northeast excavation sector (Fig. 2).[17] Digging in 2004–2008 revealed, however, not one building but a sequence of five tightly superimposed structures, identified as Buildings A–E, dating from the beginning of the Late Bronze Age to the Early Iron Age (ca. 1600–900 B.C.; Figs. 5–7). Flanking these buildings to the west was road 1, with a NNE–SSW orientation. The road had 13 closely spaced, successive pebbled surfaces reaching a maximum thickness of 0.80 m; it had been covered in LH IIIC Early to Middle with fallen blocks and cobbles (Figs. 5a, 5b). For this reason road 1 appears in squares R2, R5, R8, and R9 of the resistivity map as a broad black band.

About 30 m north of Buildings A–E, in squares R5 and R7, the outline of a squarish structure is visible. This anomaly was not excavated because of a land dispute. Some 50 to 60 m to the south of Buildings A–E, in squares R22, R23, and R24, the resistivity survey detected a configuration that suggested a double row of large rooms running WNW–ESE. This feature could not be excavated systematically, because it straddled two large land plots that we could not afford to expropriate. In 2008, however, we received permission to dig an exploratory trench of 7.5 × 5 m (trench LR770) in

Figure 4 *(opposite)*. Resistivity distribution map of the northeast sector of the islet. Darker areas depict areas of greater resistivity. No absolute gray scale can be used because of grid edge matching, interpolation, and compression applied to data. G. N. Tsokas, P. I. Tsourlos, A. Stampolidis, G. Vargemezis

15. The 2005 processing sequence for the resistance data was the following: (1) transfer of the local coordinate system of each grid to the 1987 Hellenic Geodetic Reference System (HGRS87); (2) statistical analysis of the data; (3) despiking by median filter (3 × 3 windows); (4) edge matching by stitching the left side of grid squares R29 and R30 to the right side of grid squares R33 and R34, respectively; (5) interpolation in the X and Y direction by cubic splines; (6) edge matching by stitching the top side of grid square R29 to the bottom side of GR31; (7) interpolation for the second time.

16. Scollar, Weidner, and Segeth 1986, pp. 626–630. Only two small areas in grid squares R4 and R23 were not surveyed because of the presence of dense heaps of stones. These areas are shown as blanks in Fig. 4.

17. Van de Moortel and Zahou 2003–2004; Van de Moortel 2007, 2009; Van de Moortel and Zahou, forthcoming.

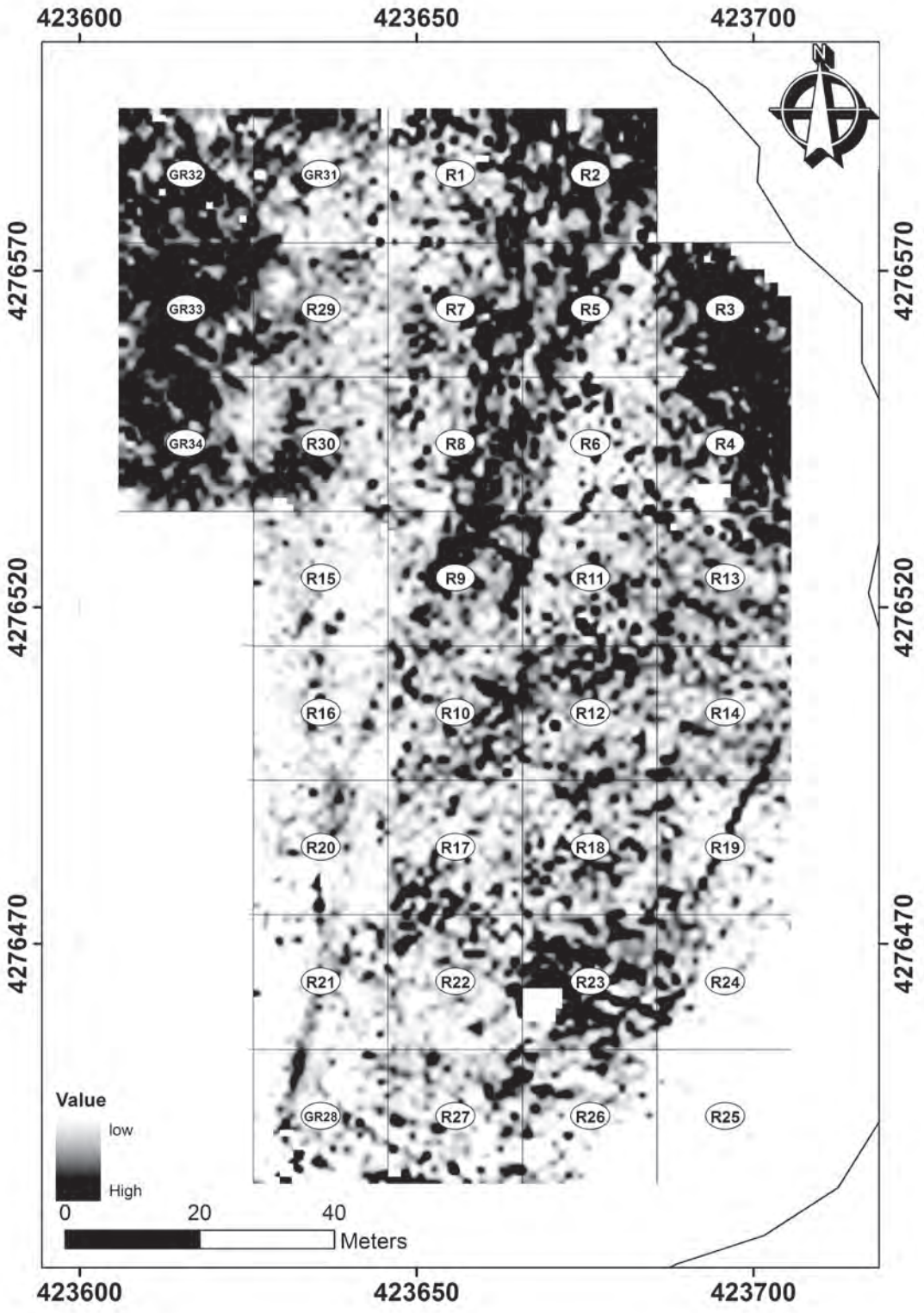

the south-central part of geophysical square R23, where we uncovered the two southernmost parallel WNW–ESE walls in the locations indicated by the resistance survey (Figs. 8–10). It is thus reasonable to assume that other dark linear anomalies forming geometric shapes on the resistance map indicate the presence of buried features.

Figure 5a. Balloon image of the northeast excavation sector at the end of the 2007 excavation season, with overlay of trenches at the east and south edges excavated in 2008 (geophysical grid squares R8, R9, and R11 in Fig. 4). The fallen building blocks in road 1 west of Building D (corresponding to the west half of grid square R9) are visible, but most of the cobbles of the LH IIIC Middle to PG road surface have been removed. Photo K. Xenikakis; overlay A. Van de Moortel

Figure 5b. Balloon image of the area of Building D in 2009, with overlay of trenches at the east and south edges excavated in 2008. The LH I and LH IIB architectural features of Building D as well as Built Chamber Tomb 73 and its LH I dromos are now exposed. The fallen building blocks on the LH IIIC Early–Middle surface of road 1 have been removed together with the three uppermost pebbled surfaces, and two deep soundings have been made in the road down to LH I and MH levels. The circular feature in the road is an excavated PG water pit. Photo K. Xenikakis; overlay A. Van de Moortel

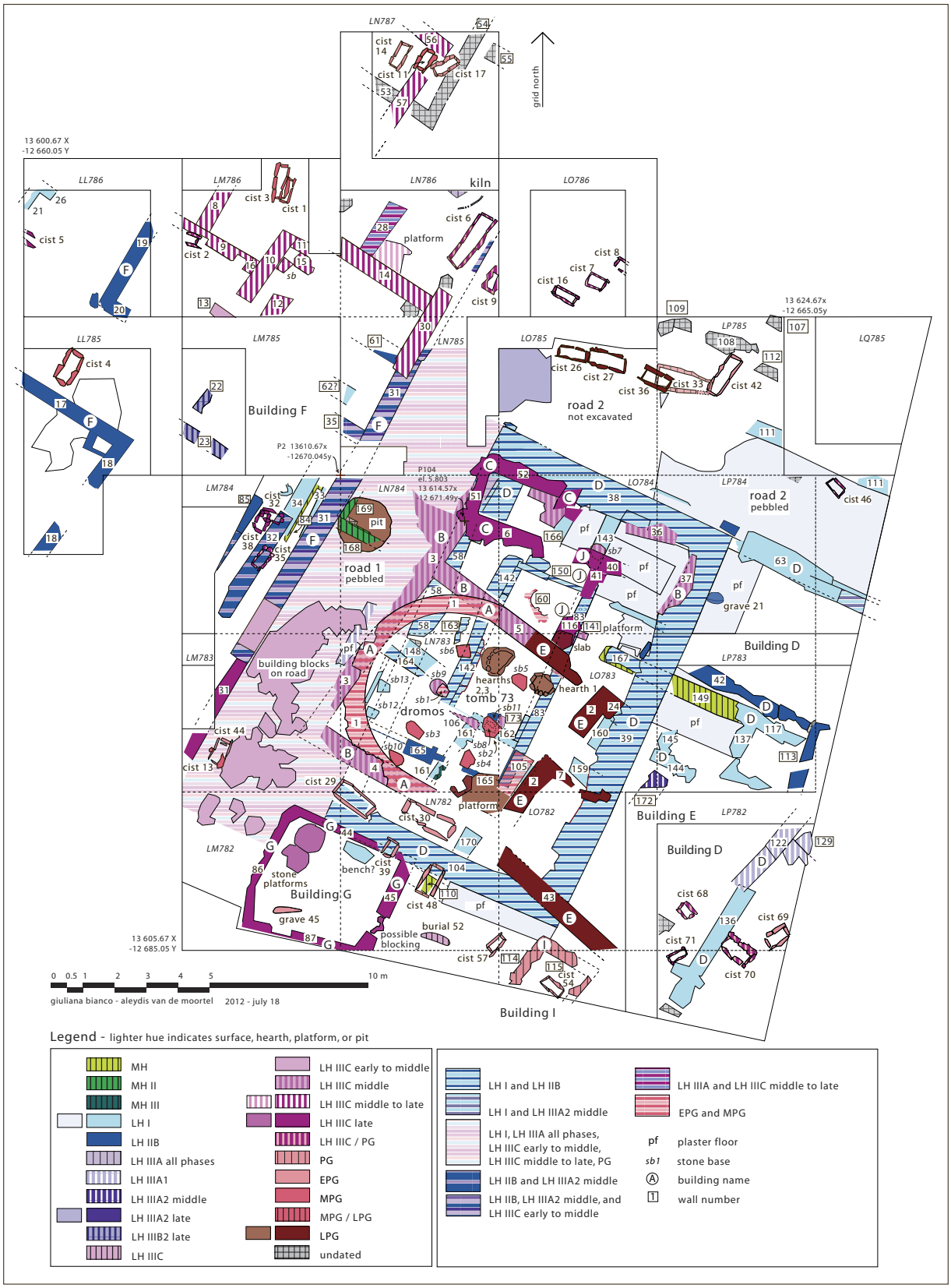

Figure 6. Site plan of the northeast excavation sector of Mitrou in 2009.
G. Bianco and A. Van de Moortel

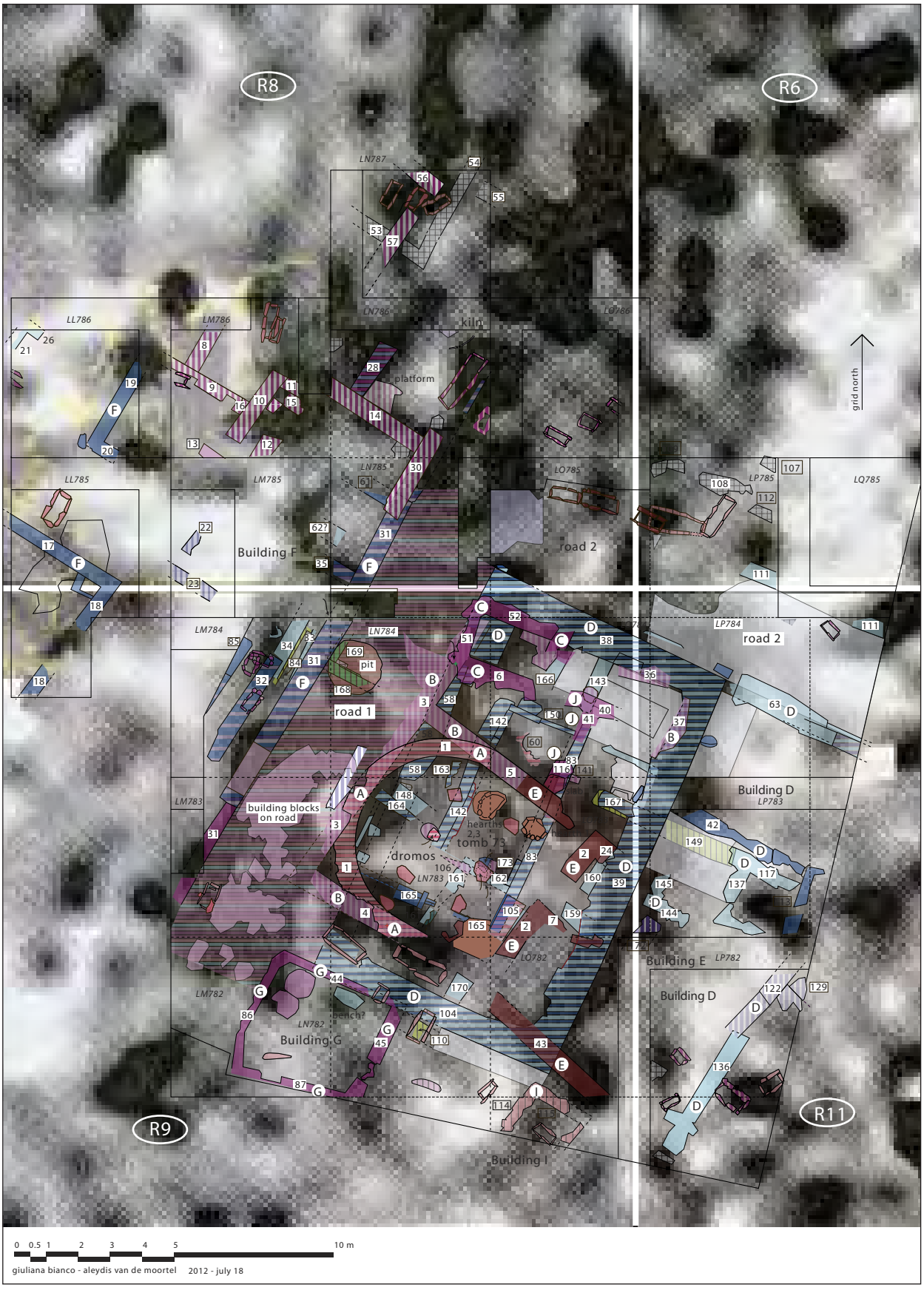
R8
R6
R9
R11
LN787
LN786
LO786
LL786
LM786
kiln
platform
grid north
LL785
LM785
LN785
LO785
LP785
LQ785
Building F
road 2
LM784
LN784
LP784
road 1
pit
building blocks on road
LM783
dromos
tomb 73
hearths 2,3
LN783
Building D
LP783
Building E
LP782
LO782
LM782
LN782
bench?
Building G
Building I
0 0.5 1 2 3 4 5 10 m
giuliana bianco - aleydis van de moortel 2012 - july 18

Figure 7 ***(opposite)*****. Wall plan of the northeast excavation sector superimposed over the 2003 electrical resistivity results. For legend, see Figure 6.** Resistance map G. N. Tsokas, P. I. Tsourlos, A. Stampolidis, G. Vargemezis; overlay G. Bianco

Figure 8. Balloon image of trench LR770, located in the east-central part of the islet (geophysical grid square R23) at the end of the 2008 excavation season. Photo K. Xenikakis

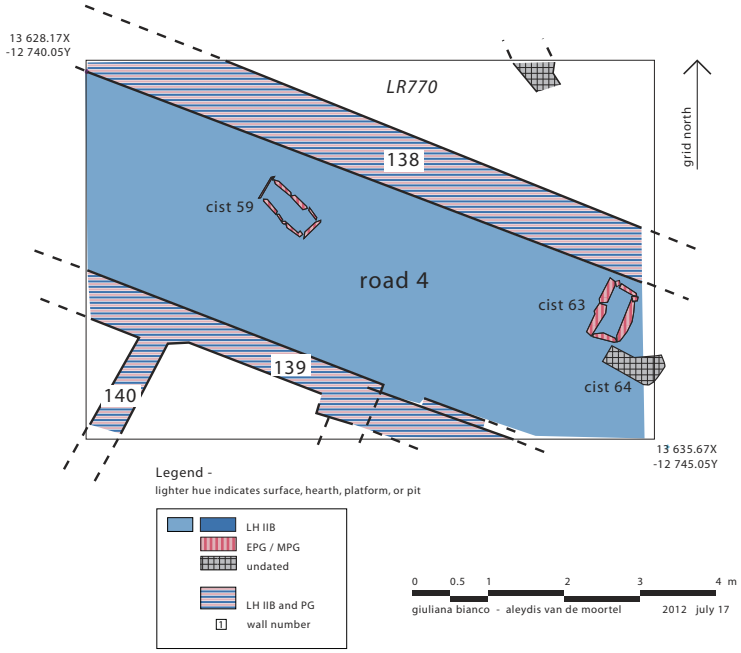

Figure 9. Site plan of trench LR770 in 2008. G. Bianco and A. Van de Moortel

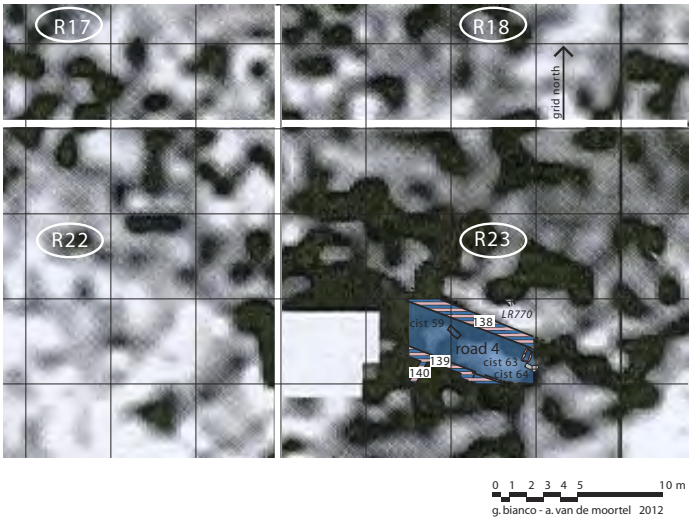

Figure 10. Wall plan of trench LR770 superimposed over the 2003 electrical resistivity results in grid squares R17, R22, and R23, showing the outlines of a long rectangular buried structure. Resistance map G. N. Tsokas, P. I. Tsourlos, A. Stampolidis, G. Vargemezis; overlay G. Bianco

The absence of linear anomalies in the resistivity map, however, does not necessarily mean that no walls are present in the subsurface. Our excavation revealed a number of walls that did not appear in the resistivity survey, even though their uppermost surfaces were located only ca. 0.20 to 0.30 m below the present surface—well within the 0.75–1.00 m range of the survey (e.g., walls 2, 6, 8, 9, 22, 23, 44, 86, and 87; cf. Figs. 4, 6, 7). While the reason for this discrepancy is still under investigation, we may observe that nearly all of these walls are less than 0.55 m wide. The only undetected wall that is thicker—west wall 2 of Building E—measures just 0.60 m wide and has two sections: its southern part was found in poor condition, whereas its northern part was sound but extended only 1.6 m long north–south. It is not yet clear why the northern section was not reflected in the resistivity measurements, which were taken in east–west transects 1 m apart.

At the northeastern edge of the surveyed area, in grid squares R2, R3, and R4, appear several resistance anomalies in the form of dense black patches with a rather irregular shape. It is conceivable that these patches indicate concentrations of stones in the subsurface that are the remains of walls that collapsed or were destroyed in antiquity. It seems more likely, however, that they represent bedrock, because in the adjacent eastern sea scarp of the islet bedrock is visible less than 1 m below the present surface. It is also possible that the patches represent piles of stones accumulated by later farmers clearing their fields. This explanation is less plausible, however, because it is unlikely that farmers would have retained such a large, dense collection of rocks on their fields rather than throwing them down the cliff.

MAGNETIC GRADIOMETRY

As noted above, resistance mapping is not well suited to the western and southern sections of Mitrou, which are covered with olive groves; tree roots can skew the accuracy of resistance mapping by generating pockets of high resistivity. Thus we used magnetometry to survey these portions of Mitrou. Magnetic prospecting is currently one of the main tools used for locating and mapping concealed ancient features. The earth's magnetic field is precisely recorded in great spatial detail. Antiquities in the subsurface disturb the magnetic homogeneity of the earth, creating detectable anomalies in the survey data.[18] Because exposure to high heat and subsequent cooling can permanently magnetize objects, magnetic prospecting is a powerful tool for detecting kilns, ovens, hearths, and features containing a large amount of burned clay. Magnetometry is also an effective method for delineating soil features such as ditches, pits, and trenches, and it can be used to produce anomalous magnetic field maps reflecting weakly magnetized structures such as wall foundations, yielding images of architectural remains comparable to those created by resistance mapping.

18. Aitken 1974, pp. 214–234; Scollar, Weidner, and Segeth 1986, p. 624; Clark 1990, pp. 64–66, 78–83.

Methodology

A magnetic survey is carried out in the field in a manner similar to resistance mapping. Measurements are taken along parallel traverses, but at shorter distances than in a resistivity survey. We placed measuring tapes on the ground at 0.5 m intervals to form a subsidiary grid within each grid square; the intersections of the tapes indicated where the measurements should be performed. In each 20 × 20 m grid square, we took 1,600 readings—four times the number of resistance measurements recorded in a grid square. Yet the magnetic survey proceeds relatively quickly, as there is no need to insert probes into the soil for each reading and the operator simply carries the instrument from intersection to intersection on the grid of tapes laid out within the grid square. Although the area covered by the magnetic survey in June 2005—42 grid squares including ca. 16,800 m^2 of land surface—was greater than the area of the resistivity survey (13,600 m^2), it was completed in the same amount of time, four days.

Among the various magnetometric methods in use today, magnetic gradiometry is widely practiced in place of the traditional total magnetic field method. In gradiometry, two magnetic sensors are placed on top of one another at a fixed distance, so that the field's magnetism can be measured at two different heights simultaneously. The readings at the two heights are subtracted, yielding mathematically the first vertical difference of the magnetic field, which is an approximation of its vertical gradient. Because the earth's magnetic field is not static but changes continually even within the course of a single day, any magnetometric method must correct for these variations. The advantage of gradiometry is that since measurements are taken simultaneously at two different heights at each position of the grid, the problem of temporal magnetic variation in the field is automatically eliminated.

Like resistivity surveying, magnetic gradiometry provides an image of the spatial distribution of the magnetic field, in which anomalies indicate buried magnetic structures.[19] (Nonmagnetic features will also appear as anomalies if they are surrounded by a magnetic medium, such as clayey soil with an enhanced magnetic profile.) Magnetic data are more complex than electrical resistance data, however, because of the bipolar nature of the magnetic field. The ruins of a wall, for example, create a bell-shaped electrical resistance anomaly centered exactly over it as well as a magnetic signal with both positive and negative lobes. The magnetic field observed at the surface is the superposition of the fields created by all magnetic objects in the vicinity; consequently, interpretation of the magnetic data is more difficult if the anomalies caused by buried structures are weak and superimposed on one another. The processing of the data and presentation of the results are done in a similar way as in resistance mapping, except that some special treatment is initially needed because of the different nature of the data.

In each square of the survey grid at Mitrou, magnetic measurements were taken with a gradiometer at 0.5 m intervals along traverses spaced 0.5 m apart.[20] It is difficult to specify the depth to which anomalies can be detected because this is a function of the contrast in susceptibility between

19. Becker 1995, pp. 220–224.

20. The FM256 fluxgate gradiometer manufactured by Geoscan Research was used.

the target and its surroundings as well as its depth and dimensions. As a rule of thumb, for the kind of structures buried at Mitrou magnetic anomalies can be detected to about 1.50 m below the surface. Variations in orientation and the calibration of the instrument were checked after the completion of each four grid squares. Data were downloaded onto a laptop computer in the field each time eight grid squares had been measured. This approach enabled a quick check on data quality in situ. Additional data checks as well as initial data processing were performed at the end of each day of fieldwork. After the completion of the survey, data processing continued at the Laboratory of Exploration Geophysics at the Aristotelian University of Thessaloniki.[21] Finally, we created grayscale images that presented the spatial distribution of the processed magnetic gradients in a form resembling the site plan of an excavated area.

Results of the Magnetic Survey

In the resistivity survey, we found that the location of resistance anomalies—areas of higher resistance—corresponded to the location of building stones and bedrock as revealed by excavation and observation of the scarps on the northeast shore of the islet. Our assumption that buried stone structures would yield weaker magnetic signals than the surrounding soil was confirmed by magnetic susceptibility measurements conducted on samples of soil and stone masonry material found on the surface of the site (Table 1).[22] It is evident from Table 1 that a pronounced difference of susceptibilities exists between the topsoil and the main material (limestone) used for building.

TABLE 1. MEAN VALUES OF MAGNETIC SUSCEPTIBILITY MEASUREMENTS (VOLUME)

Material	*Samples*	*Mean (SI units)*
Stones (masonry material), limestone	10	5×10^{-5}
Stones (masonry material?), diabase (ultrabasic components)*	4	10×10^{-4}
Soil (near surface stratum, topsoil)	20	25×10^{-4}

*The samples also show a strong component of remanent magnetization.

In Figure 11, the images obtained from both the magnetic survey and the resistance survey have been superimposed on an aerial photograph of the islet. Areas of high resistance are indicated by darker shades of gray,

Figure 11 *(opposite)*. **Results of resistance and gradiometry mapping superimposed on an aerial view of the islet. Position of the grid with respect to the ground surface is slightly distorted due to the oblique angle of the aerial photograph. Darker shades indicate stronger anomalies. No absolute values can be displayed because two types of data are plotted, and edge match corrections as well as dynamic range compression have been applied separately for each data set. Coordinates follow the Hellenic Geodetic Reference System of 1987.** Balloon photo K. Xenikakis; overlay G. N. Tsokas, P. I. Tsourlos, A. Stampolidis, G. Vargemezis

21. The processing sequence was decided after various tests and included the following steps: (1) transformation of the local coordinate system of each grid to the Hellenic Geodetic Reference System of 1987 (HGRS87), i.e., the mesh of the geophysical cells and each measurement were referenced; (2) statistical analysis of the data; (3) despiking by median filter, performed in 3×3 windows of the data, after which the filtered data were visually checked against the originals to ensure that no useful information was discarded; (4) transfer of the mean of each traverse to zero (Zero Mean Traverse); (5) interpolation both in the X and Y direction using cubic splines of the form sinX/X; (6) smoothing by low-pass Gaussian filter; (7) clipping of the dynamic range to relatively low values (-5 to 5 nT/m) to enhance the effect of weak anomalies caused by the antiquities at the expense of the strong ones caused by ferrous objects near the surface. The latter are either iron litter or manmade features (pipe, reinforced concrete piles, etc.).

22. "Magnetic susceptibility is a measure of the degree to which a substance may be magnetized" (Sheriff 1981, p. 191). The magnetic susceptibility measurements were performed using a JH-8 κ-meter from GeoInstruments.

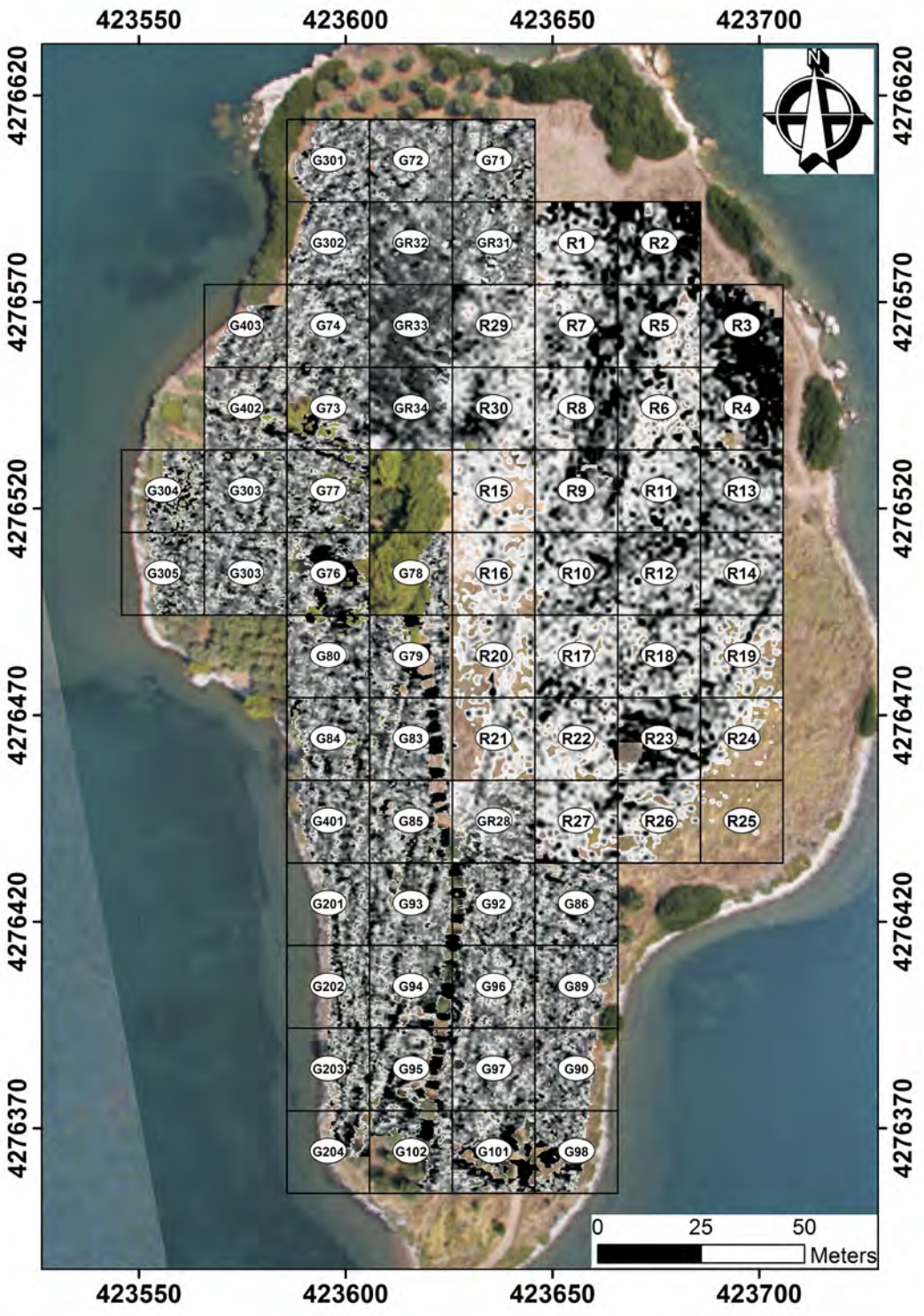

but the scale of the magnetic readings has been inverted: low values are dark and higher ones are paler. Thus magnetic anomalies, indicated by lower values, and resistance anomalies, indicated by higher values, are both represented as darker shades of gray on this map.

Figure 12 presents a detailed interpretive map of the buried ancient constructions causing the anomalies represented in Figure 11. It is clear that almost the entire area of the islet contains antiquities. As in the results

Figure 12. Interpretive plan of all anomalies recorded by resistance and magnetic mapping. Key: (1) modern water pipe; (2) anomaly detected by Steven Soter; (3) undulating plow marks; (4) ancient structures; (5) remains of roads 1–4, partially uncovered by excavation; (6) destroyed modern structures; (7) bedrock or dense mass of ancient structures. Coordinates follow the Hellenic Geodetic Reference System of 1987. G. N. Tsokas, P. I. Tsourlos, A. Stampolidis, G. Vargemezis

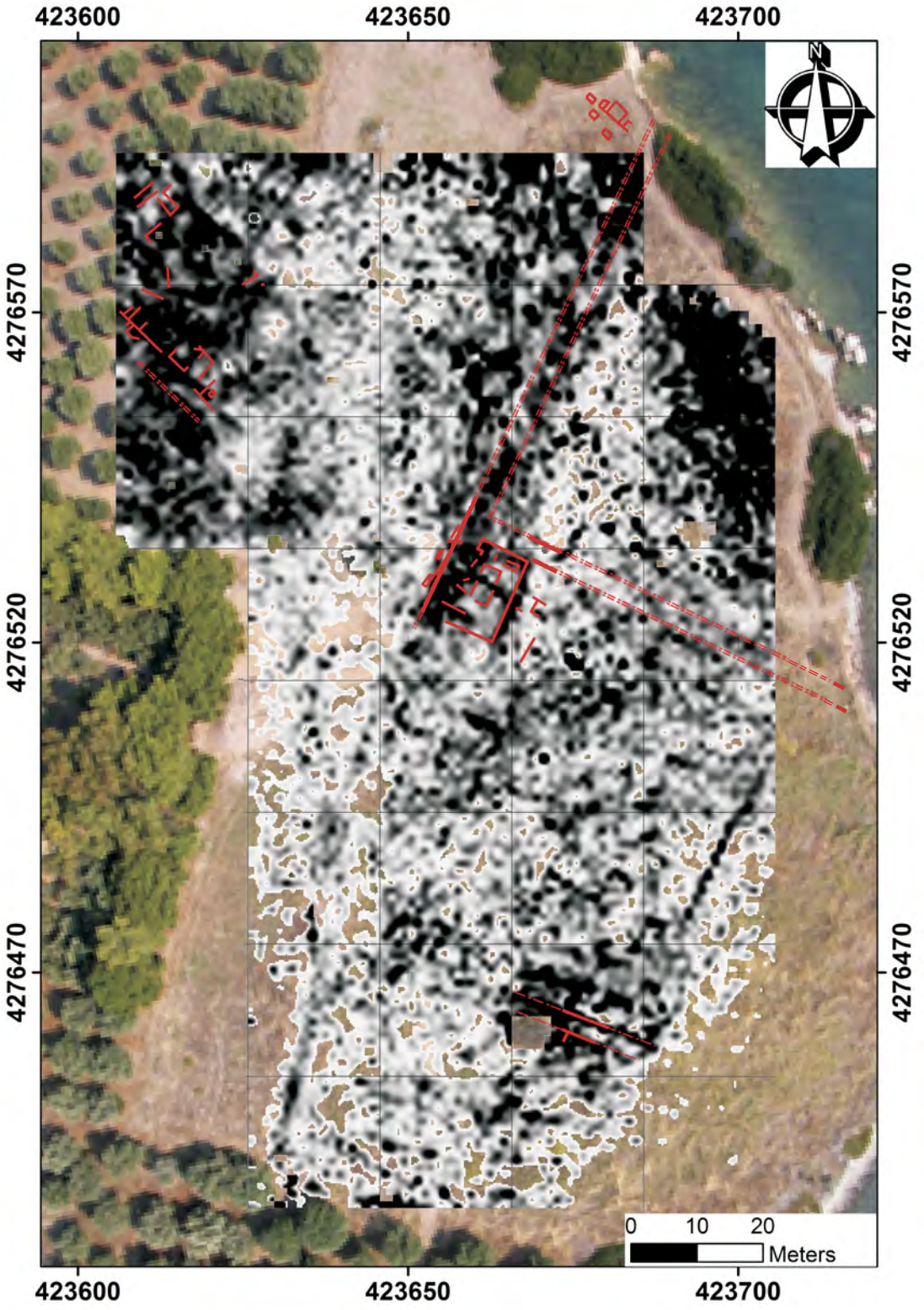

Figure 13. Outline of excavated walls and roads (in solid red) as well as hypothetical roads (in red dashes) superimposed over the resistance map and the balloon image of the islet. Balloon photo K. Xenikakis; architectural drawing G. Bianco; overlay G. N. Tsokas, P. I. Tsourlos, A. Stampolidis, G. Vargemezis

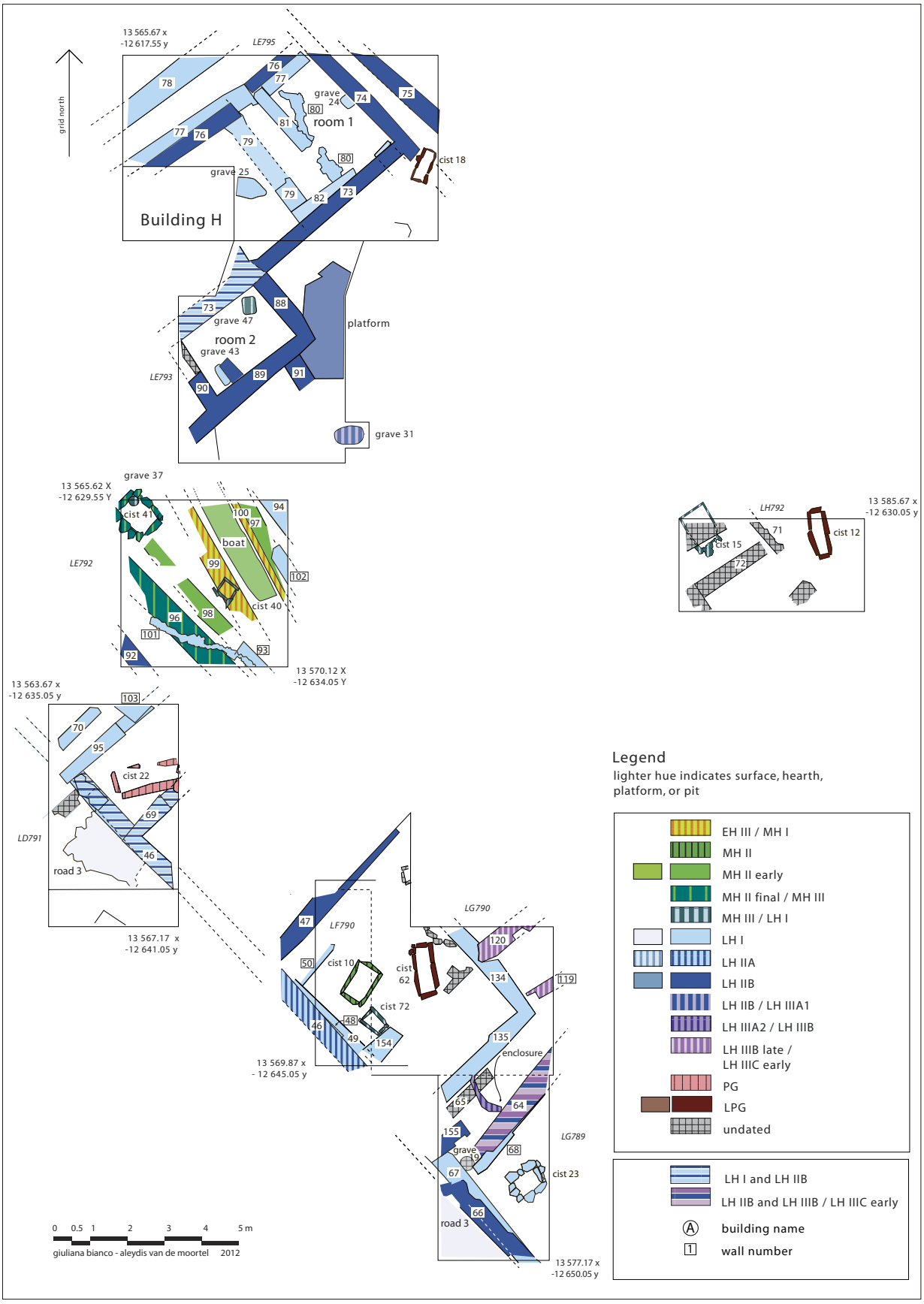
13 565.67 x
-12 617.55 y
LE795
grid north
78
76
77
grave 24
74
75
80
81
room 1
77
76
79
80
cist 18
grave 25
79
82
73
Building H
73
grave 47
88
platform
room 2
grave 43
LE793
89
91
90
grave 31
grave 37
13 565.62 X
-12 629.55 Y
cist 41
100
97
94
boat
LE792
99
102
cist 40
96
98
101
92
93
13 570.12 X
-12 634.05 Y
LH792
13 585.67 x
-12 630.05 y
71
cist 12
cist 15
72
13 563.67 x
-12 635.05 y
103
70
95
cist 22
69
LD791
46
road 3
13 567.17 x
-12 641.05 y
47
LF790
LG790
120
50
cist 10
cist 62
134
119
cist 72
148
46
49
154
135
enclosure
13 569.87 x
- 12 645.05 y
65
64
155
LG789
grave 19
68
67
cist 23
66
road 3
13 577.17 x
-12 650.05 y
0 0.5 1 2 3 4 5 m
giuliana bianco - aleydis van de moortel 2012
Legend
lighter hue indicates surface, hearth, platform, or pit
EH III / MH I
MH II
MH II early
MH II final / MH III
MH III / LH I
LH I
LH IIA
LH IIB
LH IIB / LH IIIA1
LH IIIA2 / LH IIIB
LH IIIB late / LH IIIC early
PG
LPG
undated
LH I and LH IIB
LH IIB and LH IIIB / LH IIIC early
Ⓐ building name
1 wall number

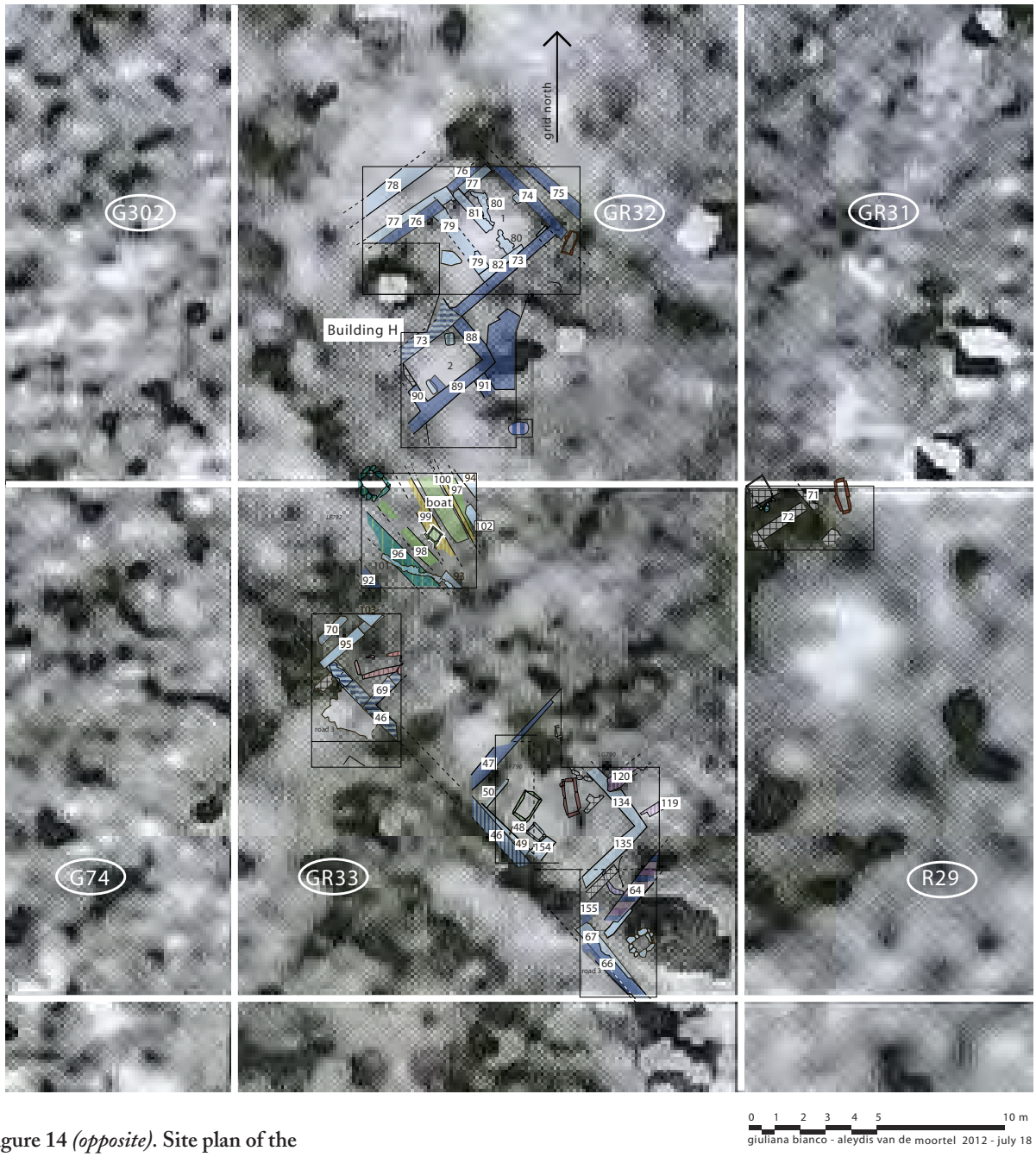

Figure 14 *(opposite)*. **Site plan of the northwest excavation sector in 2008.** G. Bianco and A. Van de Moortel

Figure 15 *(above)*. **Wall plan of the northwest excavation sector of Mitrou (2008) superimposed over the resistance and magnetometry results, which show a large anomaly of apsidal shape.** Resistivity map G. N. Tsokas, P. I. Tsourlos, A. Stampolidis, G. Vargemezis; overlay G. Bianco

of the resistance mapping, most of the constructions detected by magnetic gradiometry seem to be aligned on NNE–SSW and WNW–ESE axes, and the overall impression created is that of a dense urban complex covering most of the islet. It is evident from a comparison of the geophysical results and the archaeological plans (Figs. 6, 7, 9, 10, 13–15) that the orientation of the structures revealed by magnetic prospecting and resistance mapping coincides with that uncovered by archaeological excavation. As in the resistivity results, long linear anomalies are observed almost everywhere in the magnetometry map, possibly reflecting the presence of long walls and, presumably, roads. In some cases the alignments tend to create neat

rectangles, as in squares G72, GR34, G86, G85, and G93, suggesting the presence of concealed ancient structures (Fig. 11). At other locations, such as squares G98 and G101, the shapes of structures are not very pronounced.

In squares G302, GR32, GR31, G74, GR33, and R29, one can see the possible outline of a large apsidal structure or architectural complex, ca. 32 × 24 m in area. Most of this outline was already visible in the 2003 electrical resistivity survey. Encouraged by the results of the 2005 magnetometry survey, we opened a second excavation sector at this location in the northwest part of the islet in the hope of identifying and dating this purported building or complex. Trenches excavated over its outlines in 2005–2008 revealed a number of walls mainly of LH I and II date that correspond to the linear anomalies of the geophysical surveys (Figs. 14, 15). The finds from this area have been remarkable (see below). The anomaly's substantial size and the modest widths of most of the walls excavated inside it make it likely that it is a complex of multiple buildings rather than a single structure. The presence of olive trees has restricted the size and spatial distribution of our trenches, however, and we have not yet been able to establish the boundaries or shape of this complex.

The very strong anomaly formed by a serpentine alignment of alternating black and transparent areas running approximately south–north from square G102 to square G79 is caused by a buried modern water pipe (Fig. 11). This pipe ends at a water tap visible on the surface of square G76 next to the ruins of a modern structure of reinforced concrete. These modern features cause a very strong anomaly roughly in the center of square G76. The pipe crosses the narrow passage from the islet to the shore and emerges on the beach of Tragana. There we conducted a test, measuring the magnetic field in five traverses across the pipe. The inferred magnetic signature was exactly the same as that shown in Figure 11.

Square G304 is very noisy due to spike-like anomalies caused by ferrous metal objects scattered all over this location. Some of this litter was visible on the ground surface during the survey. Lastly, a very strong magnetic anomaly is observed in squares G98 and G101 at the southeastern corner of the islet. This feature had already been detected by a conventional total magnetic field survey conducted 20 years ago by Steven Soter, who determined that it was relatively large.[23] Soter did not provide any interpretation, and neither are we able to offer a secure interpretation at this time, in spite of the fact that our magnetic gradiometry provides by definition a higher degree of resolution than Soter's total magnetic field readings.

ELECTRICAL RESISTIVITY TOMOGRAPHIES

As described above, conventional resistance mapping produces a two-dimensional plan view that displays all areas of high resistivity present within 0.75–1.00 m of the ground surface, without, however, indicating the absolute or relative depth of the areas of resistivity. Electrical resistivity tomography (ERT) adds a vertical dimension to this two-dimensional representation by indicating the depth at which areas of high resistivity occur. This method opens up new possibilities for pre-excavation analysis,

23. Steven Soter (pers. comm.); Soter et al. 2005, pp. 305–310.

as it enables one to see the three-dimensional configuration of a buried feature as well as the depth at which it is buried. Moreover, if measurements are taken at a high enough resolution, ERT may even be able to distinguish superimposed architectural features or structures situated at different depths.

The procedure resembles ordinary resistivity mapping, insofar as each measurement requires four electrodes: two to insert a current into the ground and two to measure the drop in potential. The depth of each measurement is controlled by adjusting the electrode separation, with penetration increasing as the distance between electrodes gets larger. Measuring resistivity at a number of depths at a series of points along a straight line yields data that can be used to create a vertical cross-section of the area below the ground. A series of such traverses conducted in parallel at regular intervals provides a series of cross-sections that can be combined to form a three-dimensional model of both lateral and vertical variations in subsurface resistivity. The recent advent of automated resistivity-measuring instruments means that any combination of measurements can be easily obtained. Today electrical resistivity tomography can be utilized to explore geological drilling holes as well as the walls and floors of standing monuments.[24]

As in the case of any geophysical technique, the resistivity measurements taken in the field do not provide a direct image of the subsurface but simply record the integrated effect of the subsurface property; thus they are referred to as measurements of apparent resistivity. A certain amount of volume is sampled by each reading, and the inferred resistivity reflects an approximation of the mean resistivity of the particular volume. By taking resistivity measurements at every placement of the electrode array on the ground surface, one creates a vertical section where apparent resistivities are registered for various depths along the section. This distribution of apparent resistivities is called a pseudo-section, because it is not the distribution of the real resistivity. If the distribution of subsurface properties is complex, the obtained image does not at all resemble a clear picture of the structure of the subsurface.

Interpreting pseudo-sections involves a great amount of expertise, and even so, in cases of complex resistivity distribution accurate interpretation is not possible. In the 1990s, the advent of fast computers allowed the development of fully automated inversion algorithms capable of producing fairly accurate three-dimensional subsurface resistivity images from pseudo-sections.[25] Such algorithms are mathematically complicated and allow the three-dimensional reconstruction of any measured data set independent of the electrode arrangement. In the tomographic surveys described below, all measured resistivity pseudo-sections were inverted using a program developed by Tsourlos.[26] The inversion results presented here effectively depict the "real" subsurface resistivity. The two-dimensional inversion scheme performs an iterative optimization based on a 2.5-D Finite element modeling scheme.[27] The algorithm is fully automated and self-correcting and performs smoothness-constrained inversion.[28] The inversion procedure is accelerated by the use of a Quasi-Newton technique for updating the Jacobian matrix. All inversions produced a surprisingly low RMS (root mean square) error of less than 2%, despite the fact that the geological

24. Tsourlos, Ogilvy, and Papazachos 2004; Tsourlos et al. 2006; Tsourlos and Tsokas 2011; Athanasiou et al. 2007; Tsokas et al. 2008, pp. 48–49.

25. Dahlin 2001, pp. 1025–1027.

26. Tsourlos 1995, pp. 249–262.

27. Meju 1994, pp. 84–96; Sharma 1997, p. 236.

28. Constable, Parker, and Constable 1987.

layers and near surface features (ancient remains) in the area are quite complicated and shown fully in three dimensions.[29]

The techniques of ERT were used in several ways to explore Mitrou. We conducted two-dimensional tomographic surveys to assess the geological and tectonic setting of the islet to a relatively great depth, about 10–15 m underneath the archaeological horizons. In addition, we executed series of parallel tomographies to establish the depth and three-dimensional configuration of select architectural features whose presence was detected by resistance mapping and magnetic gradiometry. We expected that ERT would permit us to distinguish remains from different archaeological strata, insofar as they are buried at different depths. In addition, we conducted a set of very closely spaced tomographies in archaeological trenches LP783 and LP784 to explore the three-dimensional configuration of a well-shaped linear anomaly detected by resistance mapping and to plan its excavation. Finally, we executed an experimental tomography in the same location to investigate the possibility of assessing the thickness of archaeological strata.[30]

Two-Dimensional Profiles of Mitrou

In June 2005 we conducted a pair of long two-dimensional tomographies along the main axes of the islet. The north–south tomography South (TRNS) was 213 m long and the east–west tomography West (TREW) reached a length of 141 m. Figure 16 shows the location of the traverses with respect to the geophysical grid.

For the long tomographies we chose the Schlumberger array because it has a very good signal-to-noise ratio and adequate vertical resolution.[31] Forty-eight electrodes (channels) were used and the interprobe spacing was set to 3 m (a = 3 m). The maximum separation between the potential and current electrodes was n = 8, i.e., eight times the length of the potential measuring dipole (a). The length of the measuring dipole was then doubled (2a) and n varied from 6a to 14a. In this way we achieved the desired penetration depth without significantly sacrificing resolution. The overall error of the measurements is estimated to be less than 1% (as inferred from the repeatability of the readings).

Figure 17 displays the distribution of resistivity in the subsurface as inferred from the inversion of the data. The picture is similar in both tomographies. The north–south tomography shows a highly resistive formation immediately below the present surface. This formation is about 4 m thick at the northern end of the islet and gradually tapers off to the south, disappearing at about the 163 m mark. In the perpendicular transect the resistive stratum is thickest in the east and likewise tapers off gradually over the course of 105 m. Even though the east–west tomography ran through grid square R4, which we surveyed with resistance mapping and the close-set parallel tomographies described below, no direct correlations can be drawn between these data sets because the resolution of the long tomographies is much lower, masking details seen in the resistance mapping and the closely spaced tomographies.

Underneath this resistive stratum are more conductive strata. An abrupt lateral change in electric properties within these strata is evident at the 67 m

29. The RMS error is the difference between the distribution of apparent resistivities produced by a model and the distribution observed.

30. The Syscal-IRIS resistivity meter with an automated switch was employed for all the ERT measurements of 2005. The multicore cables used were custom-built by the Laboratory of Exploration Geophysics of the Aristotle University of Thessaloniki.

31. For the two long tomographies we designed the resistivity survey to take several factors into account: the resistivity was expected to show a rather smooth lateral variation based on our inspection of the geological map of the islet; the investigated depth had to be greater than 10 m; and the difference in elevation between the extremities of the north–south traverse was about 7 m, while that of the east–west traverse was about 3 m.

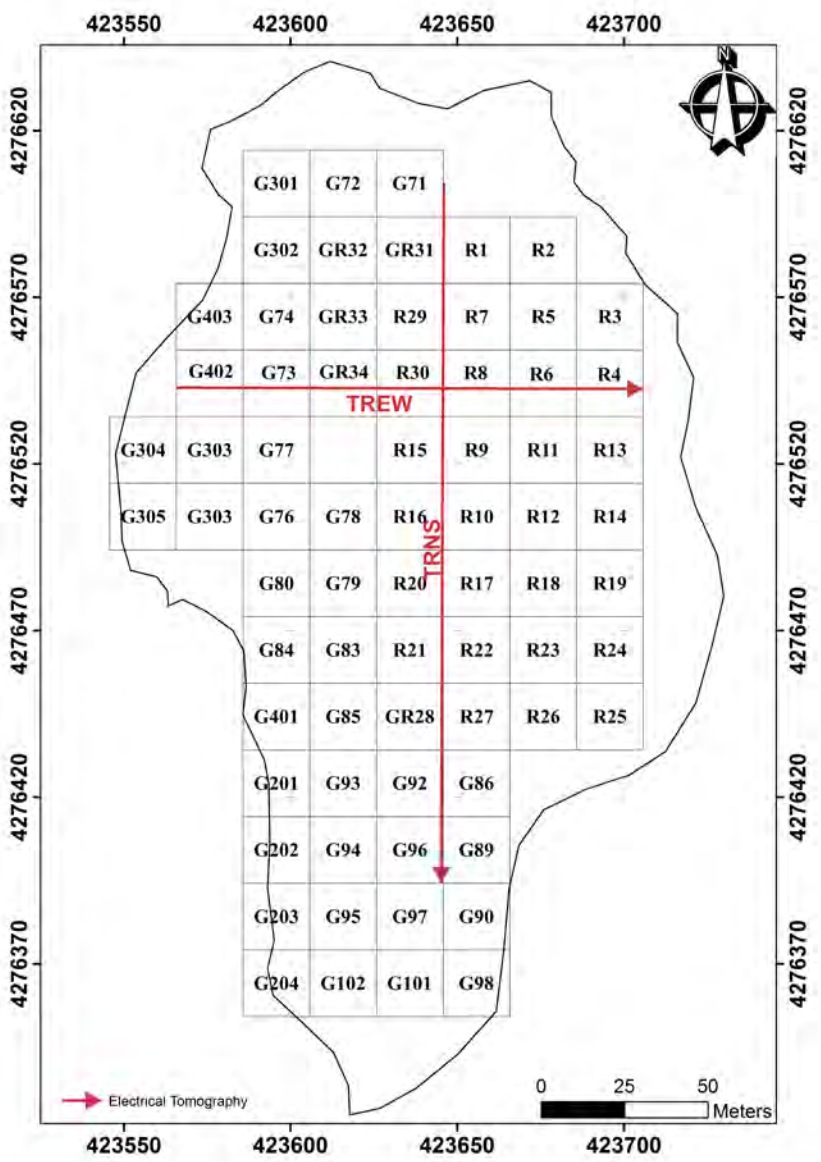

Figure 16. Location of the two traverses along which resistivity tomographies were performed in 2005. They were designed to penetrate 10–15 m below the surface. Coordinates follow the Hellenic Geodetic Reference System of 1987. G. N. Tsokas, P. I. Tsourlos, A. Stampolidis, G. Vargemezis

mark of the north–south tomography. This feature is located only ca. 10 m south of the steep rise in the limestone bedrock in archaeological trench LW788, at the eastern sea scarp of the islet, east of the northeast quadrant of geophysical grid square R4; this rise in the bedrock is represented in Figure 11 by the dark patches in grid squares R4, R3, and the northeast corner of R2.[32] The geological map of the islet shows a tectonic line at approximately the same location.[33] Therefore, we can reasonably assume that a fault running diagonally ENE–WSW is responsible for this lateral change in electrical properties.

Unlike this abrupt lateral change, the difference between the resistive near-surface stratum and the underlying conductive strata cannot be securely attributed to specific geological formations because we do not yet have data from geological drilling or deep excavation at these locations. Visual observation of those geological strata would allow us to calibrate the results of the tomographies. The rock outcrops visible in the steep scarps

32. Van de Moortel and Zahou 2011, p. 297, fig. 4.

33. Institute for Geology and Subsurface Research 1965.

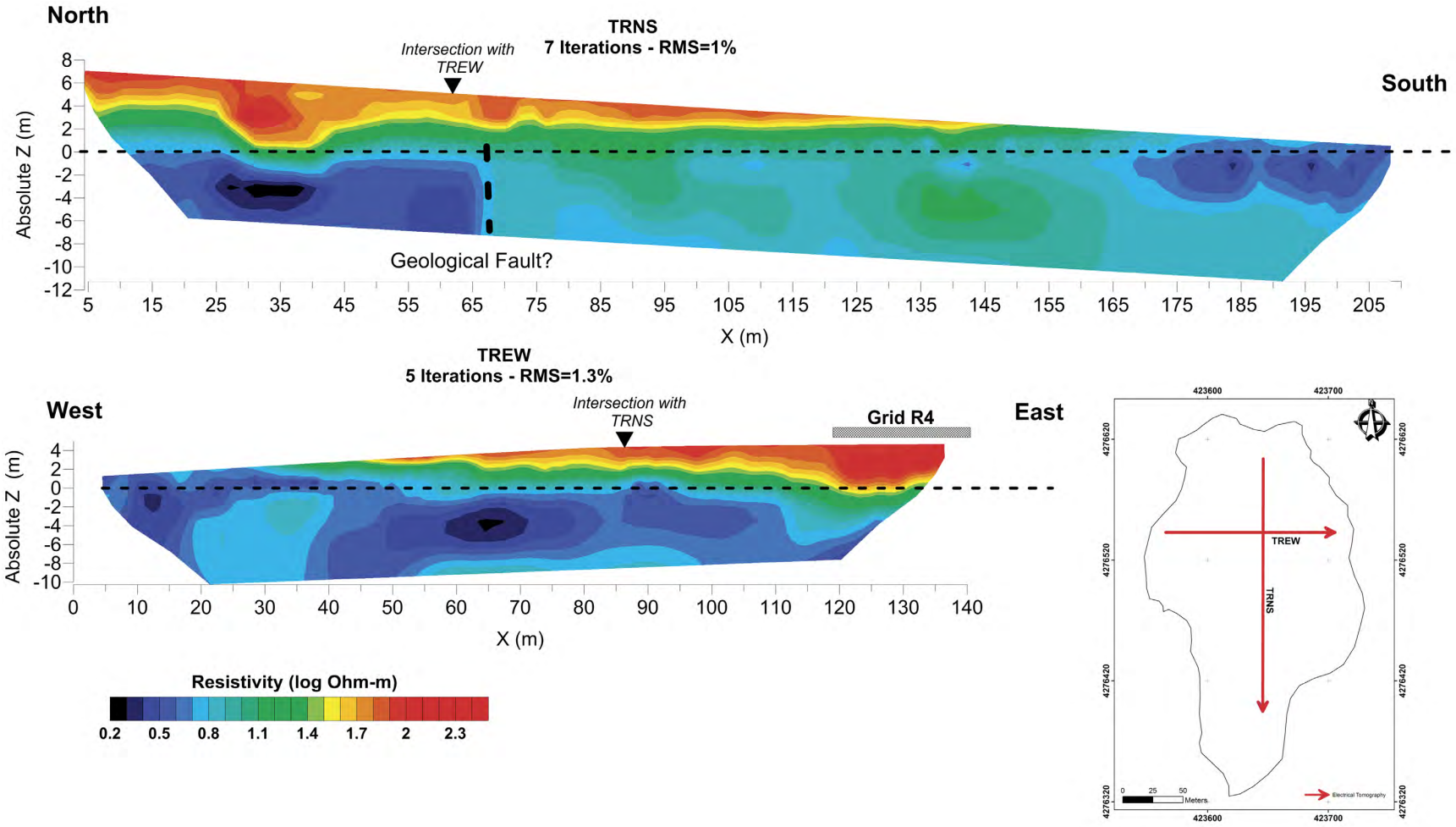

Figure 17. Inversion of the resistivity data along the long north–south and east–west transects. The dashed horizontal lines depict sea level, and a vertical dashed line indicates where the resistivities change laterally, presumably because of the presence of a fault. The intersection of the transects is marked by an inverted black triangle. G. N. Tsokas, P. I. Tsourlos, A. Stampolidis, G. Vargemezis

of the islet do not help in resolving this issue, since there is no telling how far they extend into the islet. Our understanding is impeded mainly by the presence of the unusually conductive strata that, as discussed in the next section, may represent either a thick waterlogged clayey layer of disintegrated ancient building materials or bedrock saturated with saltwater.

Three-Dimensional Images of Grid Squares R4 and R13

After the completion of resistance mapping in 2003, we conducted a three-dimensional resistivity tomography survey in squares R4 and R13 of the geophysical grid (Figs. 3, 4). These squares were chosen because promising resistance anomalies had been detected there. In all, 19 tomographies, each 20 m long, were performed in an east–west direction, along with five north–south tomographies, each 40 m long, perpendicular to the first set (Fig. 18).

For the three-dimensional survey we used a pole-dipole array, with one stationary current electrode at "infinity" and three mobile electrodes. Such an array has adequate vertical resolution and good lateral resolution, superior to that of the Wenner array.[34] Moreover, it has a good signal-to-noise ratio, which helps to ensure the accuracy of the data. The interelectrode (dipole) spacing was set to 1 m and 24 electrodes were used. The maximum dipole to current separation was eight times the dipole spacing (n = 8), so that we achieved the desired penetration depth without sacrificing lateral resolution. This particular configuration allowed a maximum penetration depth of about 3.5 m. Generally, the interval between each of the east–west sections was 2 m while the north–south tomographies were spaced 4 m apart. To avoid a pile of stones in square R4 we omitted one east–west tomography (at the 16 m mark; see Fig. 18) and one north–south tomography (at the 8 m mark). The quality of the measurements was excellent: none of them exceeded a 1% reading error when repeated.[35]

Figure 19 shows horizontal slices of grid squares R4 and R13 at seven different depths, derived from the data gathered in the 24 tomographies. The slice constructed for the depth of 0.25 m reflects the highly inhomogeneous near-surface layer disturbed by plowing. The slices constructed for the depths of 0.75 and 1.25 m clearly show linear resistive features that tend to form geometric shapes and are thus suspected to be buried walls. From the depth of 2.0 m downward no alignments are observed because they are masked by the very low resistivity of the surrounding geological formation. Comparison of the slice at 0.75 m below the surface with the resistivity map in Figures 4 and 11 shows that the outline of the rectangular structure at this shallow depth was also detected by the resistance survey of 2003. Figure 20 is a three-dimensional volume image of the subsurface distribution of resistivity in the data set used to produce the slices of Figure 19.

Since grid squares R4 and R13 are located outside the land plots slated for expropriation, we have not excavated the detected structures. Nevertheless, the three-dimensional image enhances our understanding of the ancient topography and history of the settlement. It suggests that ancient structures are preserved in at least two strata represented here at depths of ca. 0.75 m and 1.25 m below the surface, or about +5 m and +4.50 m, respectively, above sea level. Given the considerable downslope of

34. Ward 1990, pp. 174–175.

35. Measurements were taken with a SAS 400 Terrameter (ABEM) and the suitable multiplexor.

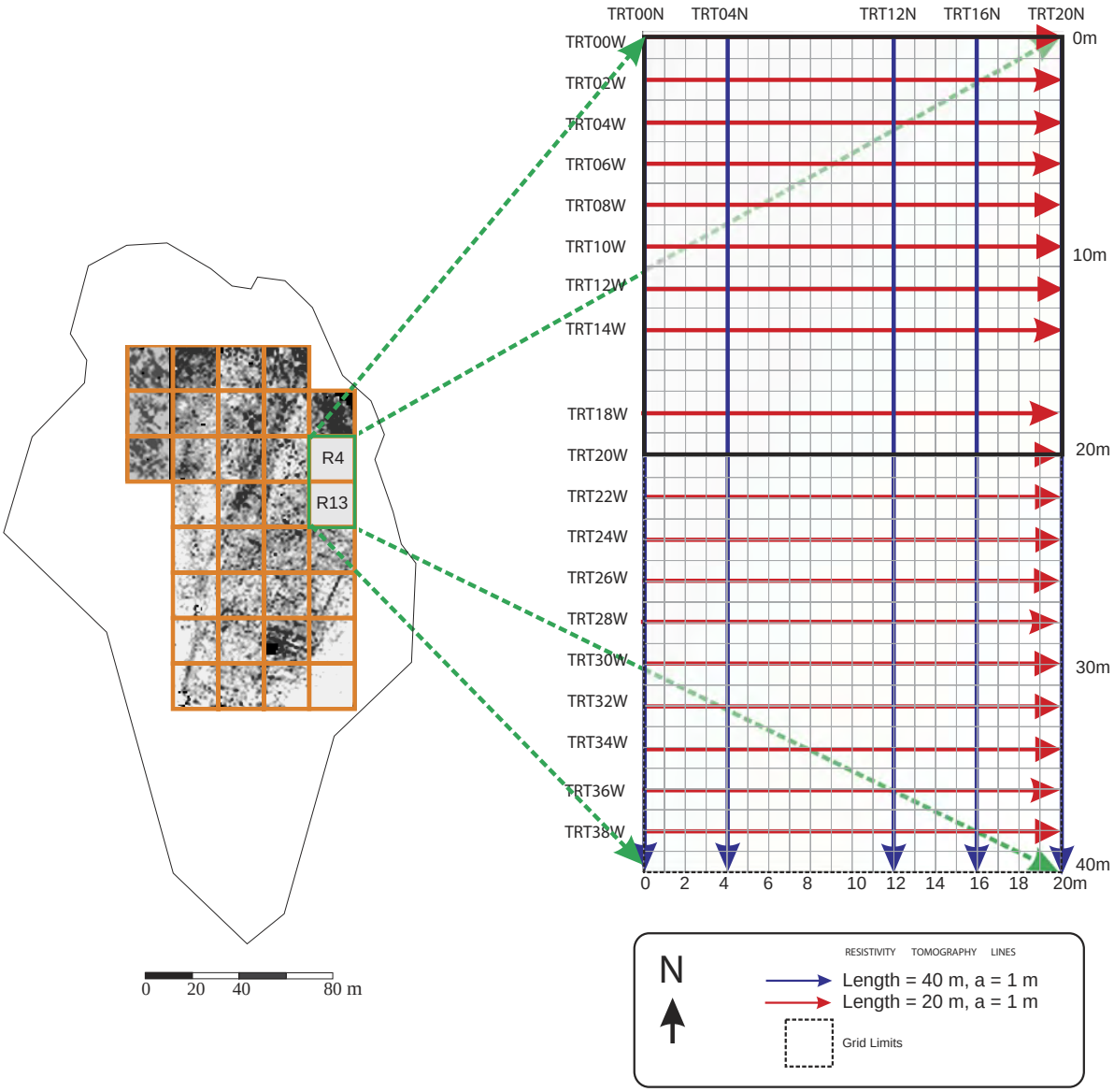

Figure 18. Resistivity tomographies carried out in 2003 in squares R4 and R13. The letter "a" denotes the inter-electrode spacing. The maximum current dipole to potential dipole separation was set to n = 8. The pole-dipole array was employed for all tomographies shown. G. N. Tsokas, P. I. Tsourlos, A. Stampolidis, G. Vargemezis

the modern and ancient surfaces from west to east in this area, it is likely that these structures are contemporary with the LH I and earlier structures uncovered at and below +4.20 masl in archaeological trench LX784, located on the eastern sea scarp of the islet some 5 to 10 m east of the eastern border of square R13. The absence of structures less than 0.75 m below the modern surface in R4 and R13 corresponds to what we found in trench LX784, and contrasts with the situation in the other excavation areas, where ancient buildings as a rule appear just 0.20 to 0.40 m below the surface. This suggests that the area of geophysical grid squares R4 and R13, like that of archaeological trench LX784, had been abandoned some time during the LH I phase (see below).

The dense inconductive (dark) layer at ca. 1.75 m below the surface in squares R4 and R13, continuing to a depth of about 2.25 m in square R4 (at roughly +4.00 to +3.00 masl), may be a thick layer of disintegrated mud brick

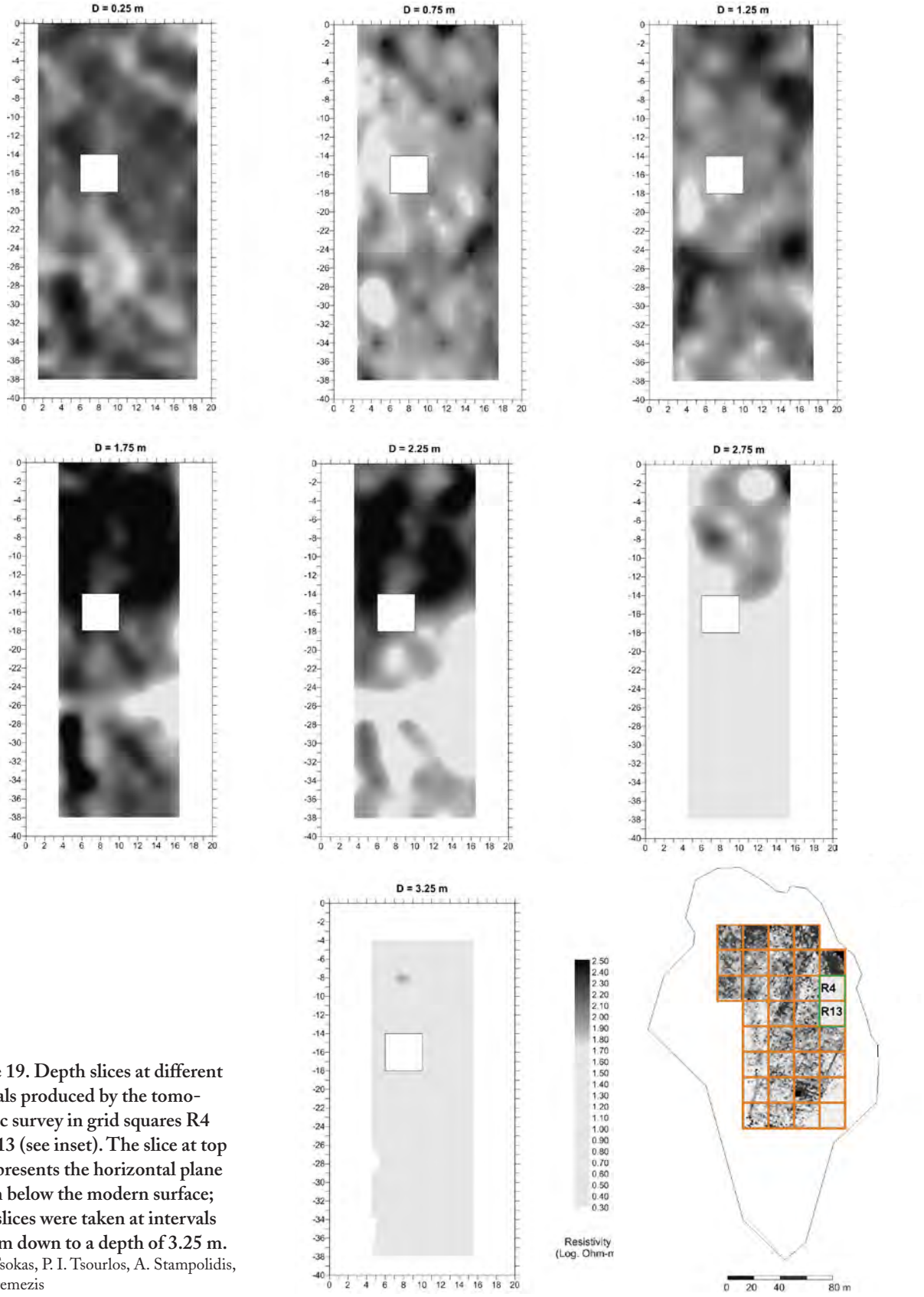

Figure 19. Depth slices at different intervals produced by the tomographic survey in grid squares R4 and R13 (see inset). The slice at top left represents the horizontal plane 0.25 m below the modern surface; other slices were taken at intervals of 0.5 m down to a depth of 3.25 m.
G. N. Tsokas, P. I. Tsourlos, A. Stampolidis, G. Vargemezis

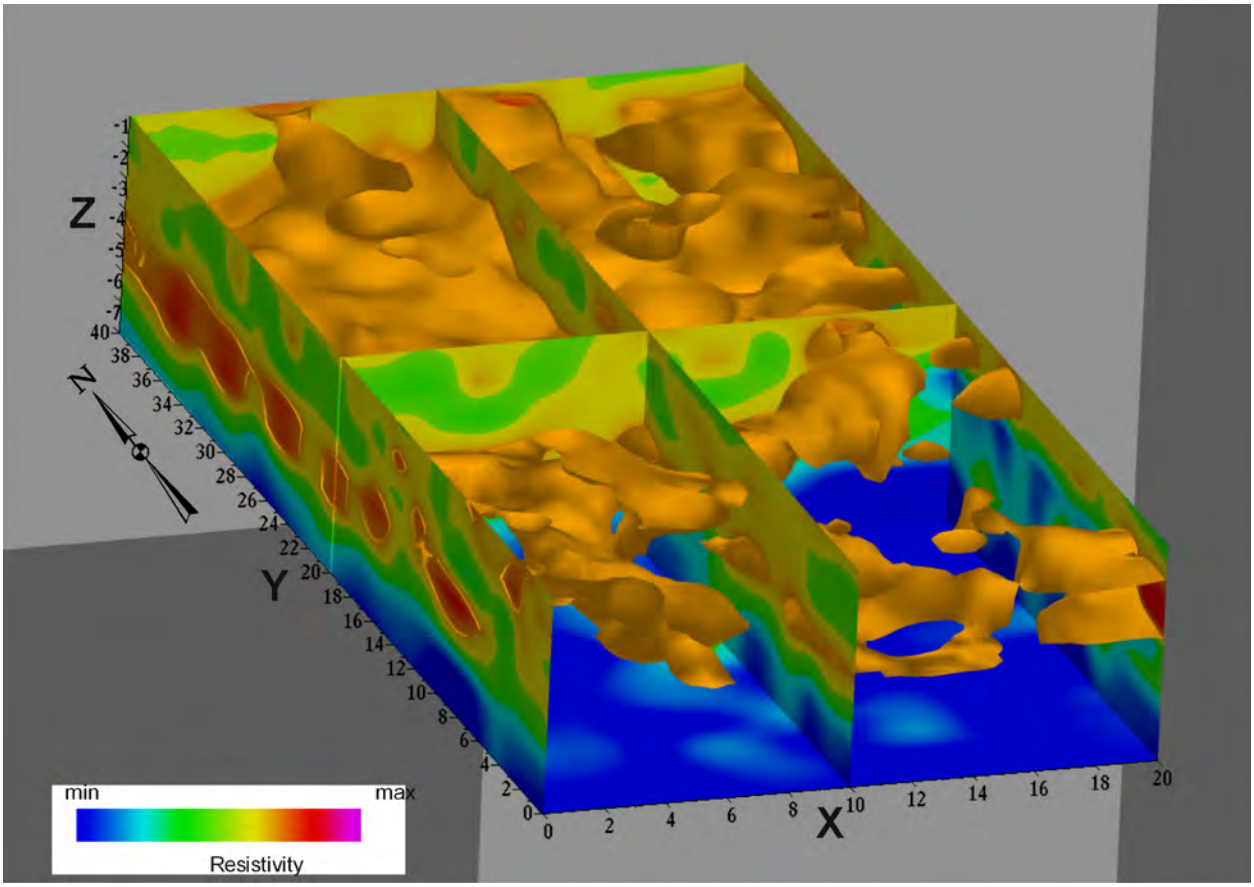

Figure 20. Three-dimensional image based on the tomographic survey in grid squares R4 and R13, showing the distribution of resistivities in the subsurface at depths down to 3.25 m. G. N. Tsokas, P. I. Tsourlos, A. Stampolidis, G. Vargemezis

and other building material (Fig. 19). The very conductive layer underneath (light gray) may consist of waterlogged clayey sediments. Strata of moist clayey earth have been encountered in Middle and Early Bronze Age levels at Mitrou, beginning at ca. 1.70 to 2.00 m below the modern surface, in all trenches that have been excavated to these depths (LE792, in geophysical grid square GR33; LN784 NE extension, in square R9; and LX784, just east of the northeast corner of square R13); they have also been observed in the east and west sea scarps. Alternatively, the dark layer seen in geophysical squares R4 and R13 could be interpreted as the top of the limestone bedrock, with the very conductive layer underneath representing limestone saturated with seawater (Figs. 19, 20). This interpretation seems less likely, however, because in nearby trench LX784 we found no bedrock; the archaeological strata went down to sea level. According to the tomographies in Figures 19 and 20, if bedrock were present in geophysical squares R4 and R13 at about +4.00 masl, then it would rise dramatically just west of trench LX784. This is not entirely impossible, since some 20 m further north at the sea scarp, in archaeological grid square LW788, bedrock rises up steeply to the north from sea level to about +4.00 m over a distance of roughly 5 m. This abrupt rise is also visible in the two-dimensional north–south tomography carried out in 2005 (see above; Fig. 17). A similarly steep rise of bedrock to the west is less likely, however, since the east–west tomography, which begins in grid square R4, shows it sloping much more gently from east to west.

High-Resolution Three-Dimensional Images in Trenches LP783 and LP784

The goal of our second resistivity tomography survey in 2005 was to produce a high-resolution three-dimensional image of subsurface resistivity distribution at a relatively shallow depth. Resistance mapping in 2003 had shown a rectilinear anomaly, thought to be the ruin of a fairly large building, in geophysical grid squares R9 and R11. We hoped to obtain a better, three-dimensional, picture of its northeast corner in trenches LP783 and LP784, located in the northwest corner of square R11.

To increase the resolution of this survey, we conducted 13 parallel north–south tomographies spaced only 0.4 m apart.[36] Figure 21 shows the grid of traverses (TR11_00) covering the 5 × 5 m archaeological trenches LP783 and LP784. As in the case of the long tomographies described above, we used the pole-dipole electrode array. Interprobe spacing was set to 0.4 m (a = 0.4 m) and one current electrode was placed a theoretically infinite distance away from the traverses (practically 40 m away). Twenty-four electrodes (channels) were used and the maximum potential to current electrode separation was again n = 8, as in the long tomographies; here too the length of the measuring dipole was then doubled (2a) and n varied from 6a to 14a.

The results of the 13 closely spaced tomographies are shown in Figure 22 in the form of horizontal depth slices. The slices at 0.1 and 0.3 m below the surface indicate thin linear anomalies, but these should not be mistaken for buried ruins. Instead they belong to the highly inhomogeneous plow zone and reflect plow marks as well as very local and spatially limited pockets of dry or wet earth. The slice at 0.5 m below the surface, however, is fully compatible with the image of square R11 produced during the 2003 resistivity survey (cf. Figs. 4, 11). The spatial distribution of resistivities at this depth creates anomalies that suggest a rectangular shape. Thus we assumed that the rectangular pattern reflects the presence of buried walls that form the northeast corner of the structure previously detected by resistivity mapping. A similar result was achieved after the full three-dimensional inversion of the data, and the inferred three-dimensional distribution of resistivities is shown in Figure 23.

In this three-dimensional image, the walls forming the northeast corner appear to be about 1.00–1.20 m wide, extending down from about 0.50–0.70 m to less than 1.40 m below the modern surface; a third, thinner, wall seems to branch off from this corner in an east-southeast direction, its upper surface lying about 0.70–1.00 m below the modern surface, or about 0.20–0.30 m lower than the upper surface of the thicker walls. Subsequent archaeological excavation indeed revealed two wall socles (walls 38 and 39) built of roughly cut fieldstones, 1.00–1.20 m wide, that form the northeast corner of a large rectangular funerary enclosure in Building D (Figs. 6, 24). East wall 39 extends down from ca. +5.40–5.30 to +4.60 masl, which is ca. 0.50–0.70 to 1.30–1.40 m below the modern surface at +6.00–5.90 m (Figs. 25, 26, below).[37] A third wall (wall 63) indeed branches off to the east-southeast. Its upper surface is quite uneven, but in the area covered by the tomography it mostly ranges between +5.10

36. The 13 parallel north–south tomographies of 2005 were carried out in an area where shallow burial depths had to be penetrated (no more than 3 m). Because we expected buried articulated architectural remains to be present in this particular location, the resistivity readings were expected to vary laterally in an intense manner.

37. The fluctuations in the depth of the walls below the modern surface reflect in part the uneven upper surface of the preserved parts of the walls and in part the unevenness of the modern ground surface, which sloped up from the southeast to the northwest and was slightly undulating, varying almost 0.30 m in elevation.

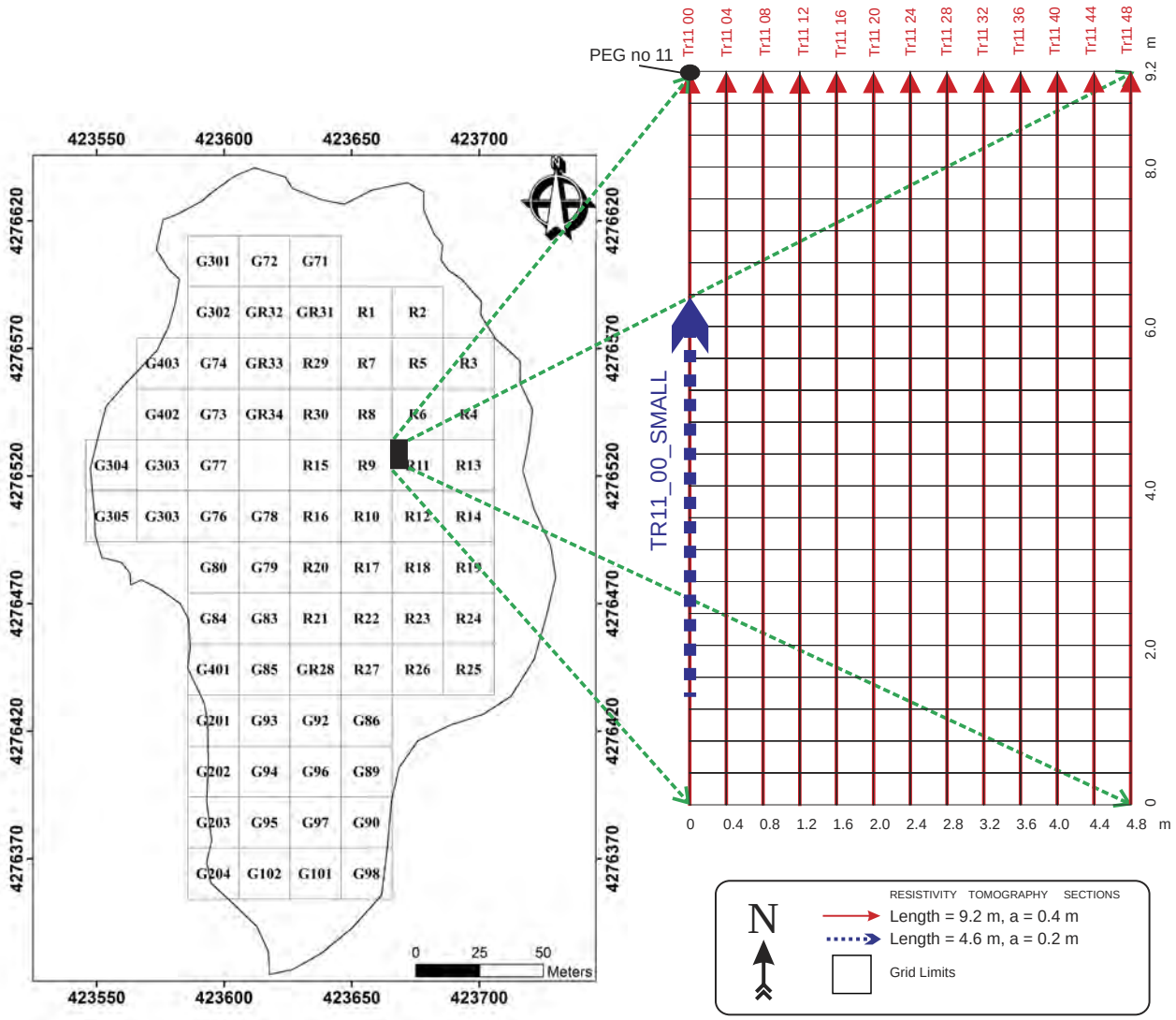

Figure 21. Layout of the grid of three-dimensional tomographies in the 5 x 5 m archaeological trenches LP783 and LP784 in the northwest corner of geophysical grid square R11. The single transect of the experimental tomography carried out with 0.2 m electrode spacing is depicted by the dashed arrow labeled "TR11_00_SMALL." The inter-electrode spacing is "a" while the maximum current dipole to potential dipole separation was set to n = 8. The pole-dipole array was used.
G. N. Tsokas, P. I. Tsourlos, A. Stampolidis, G. Vargemezis

and +5.20 masl, or about 0.20–0.40 m lower than the upper surfaces of walls 38 and 39. Thus we may conclude that the fine-grained resistivity tomography predicted the depth and configuration of the archaeological structures with remarkable accuracy. The funerary enclosure had been constructed in the LH I phase and was destroyed and abandoned in the LH IIIA2 Early subphase. The tomography even showed such detail as the thickening of the enclosure's northeast corner during the LH IIB phase by the addition of an upright wall block on the exterior (Figs. 22–24). The high resistivity patterns in the horizontal slices (Fig. 22) and the three-dimensional image (Fig. 23) extend down to a depth of about 1.7 m, where they meet an area of lower resistivity. At 2.80 m below the present surface, or ca. +3.10–3.20 masl, appear two highly conductive areas that, like those detected in squares R4 and R13 (see above), may also represent waterlogged areas.

Finally, we conducted another tomography in trenches LP783 and LP784 in 2005 with an even closer interprobe spacing, aiming to produce

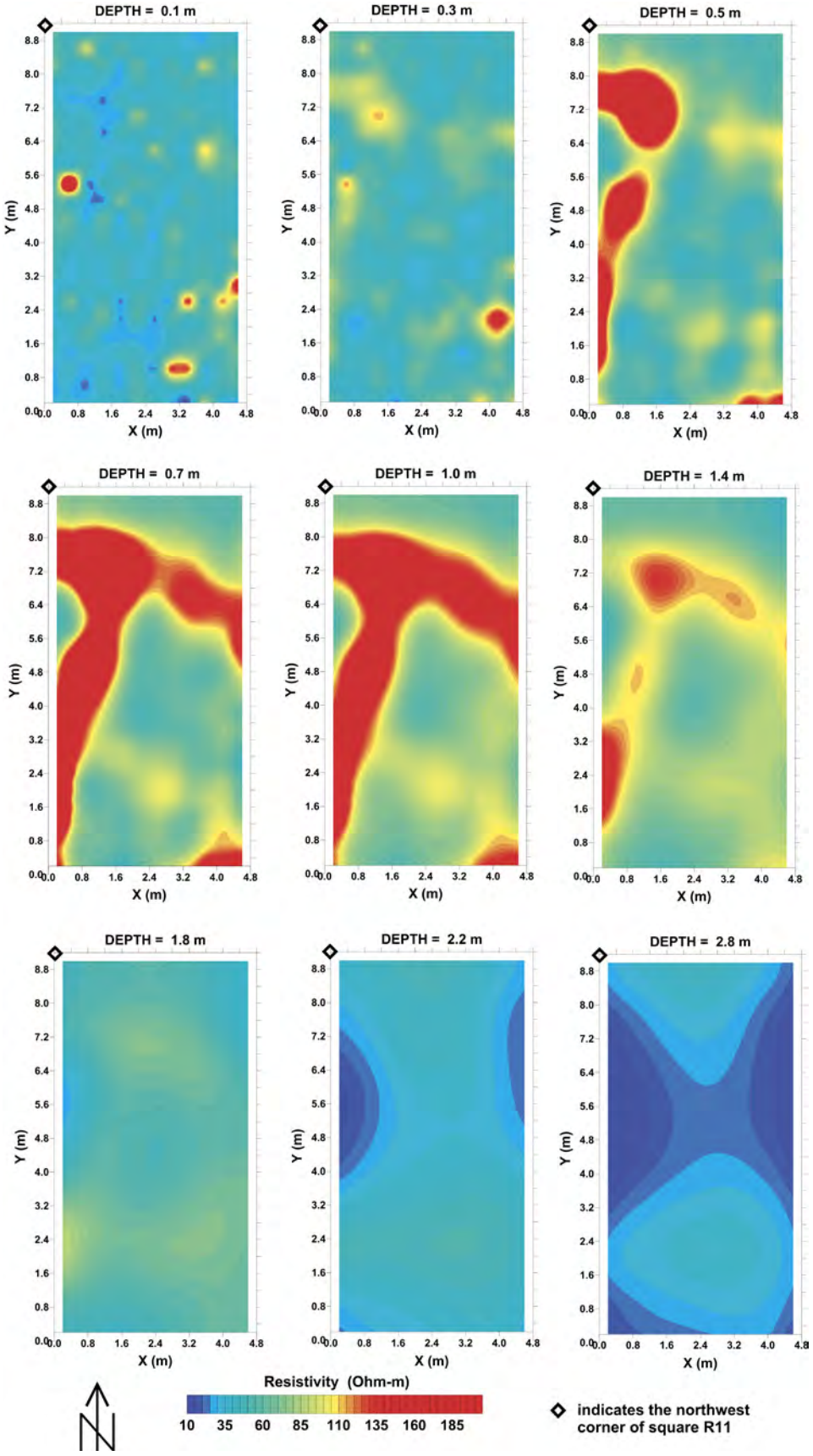

Figure 22. Result of tomographies TR11_00, spaced 0.4 m apart in archaeological trenches LP783 and LP784 in geophysical grid square R11. Depth slices are shown at selected intervals from 0.1 m to 2.8 m below the surface. G. N. Tsokas, P. I. Tsourlos, A. Stampolidis, G. Vargemezis

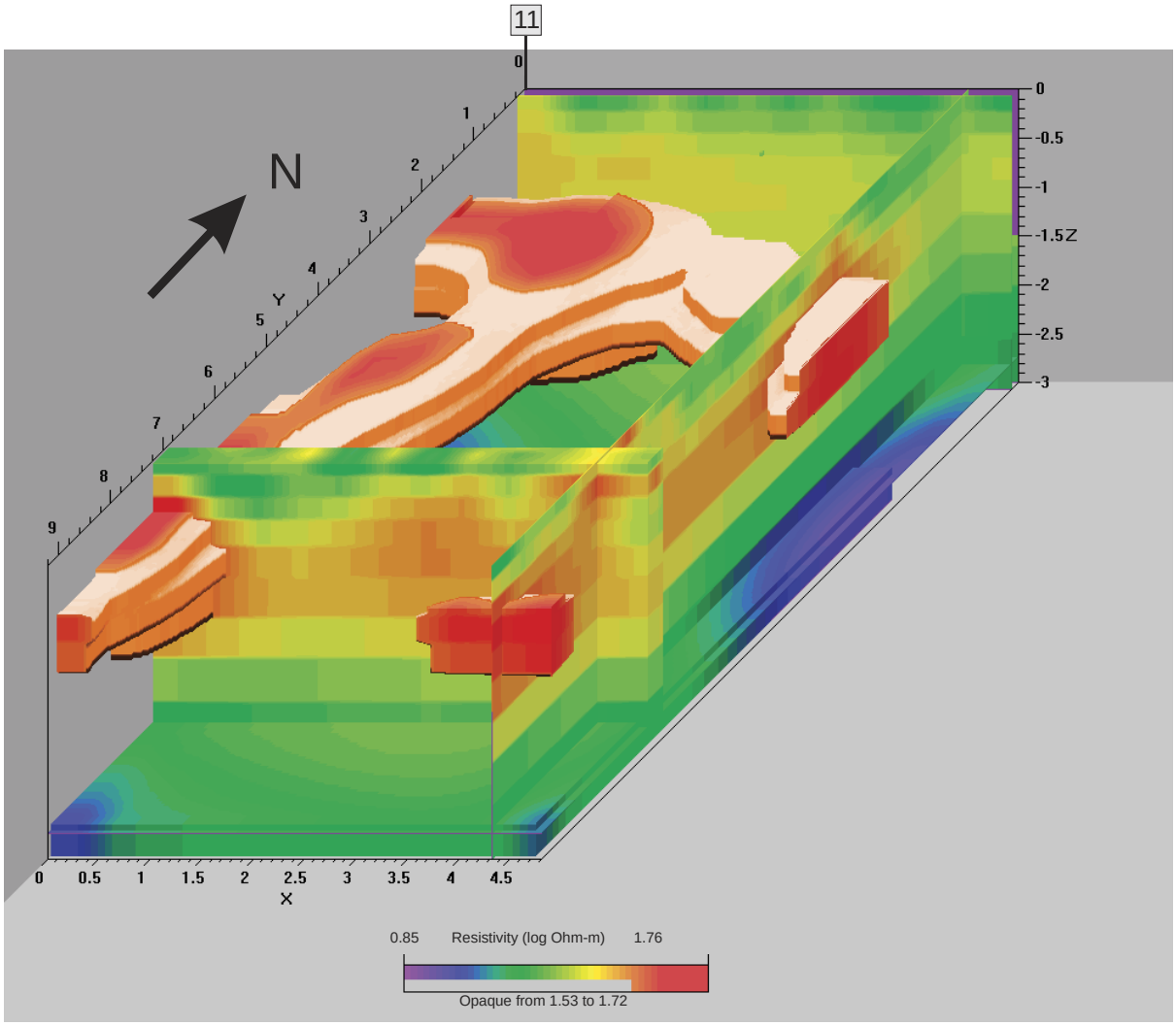

Figure 23. Result of full three-dimensional inversion of the resistivity data of the grid of tomographies TR11_00 conducted in archaeological trenches LP783 and LP784. Darker tones indicate areas of higher resistivity. The label at the top of the figure marks the northwest corner of square R11. G. N. Tsokas, P. I. Tsourlos, A. Stampolidis, G. Vargemezis

a three-dimensional image that would distinguish archaeological layers in a realistic and comprehensive manner. This survey was entirely experimental. The tomography, labeled "TR11_00_SMALL" in Figure 21, was carried out along the westernmost line of the previous tomography, TR11_00. The interprobe spacing was set at 0.2 m and a pole-dipole array was again employed. The arrangement for the maximum n, when the measuring spacing was a and 2a, was the same as for the tomographies of the TR11_00 grid. Only one transect was set out, its electrodes spaced 0.2 m apart (Fig. 21). Figure 25 shows the location of the experimental tomography with respect to the TR11_00 grid, as well as the inverted data from both TR11_00_SMALL and TR11_00. The results of TR11_00_SMALL did not fulfill our expectations of surpassing the level of detail obtained by the previous set of tomographies. The undulations of the stratum of high resistivity show exactly the same pattern as that observed in the result of TR11_00, even though the spacing of the electrodes was half that used for TR11_00 (0.2 m versus 0.4 m).

Figure 24. The northeast corner of Building D's funerary enclosure seen from the south at the end of the 2005 excavation season. Wall 38 is the north wall of the enclosure, and wall 39 its east wall. The beginning of wall 63, branching off to the east-southeast, is visible on the right.
Photo T. Dabney

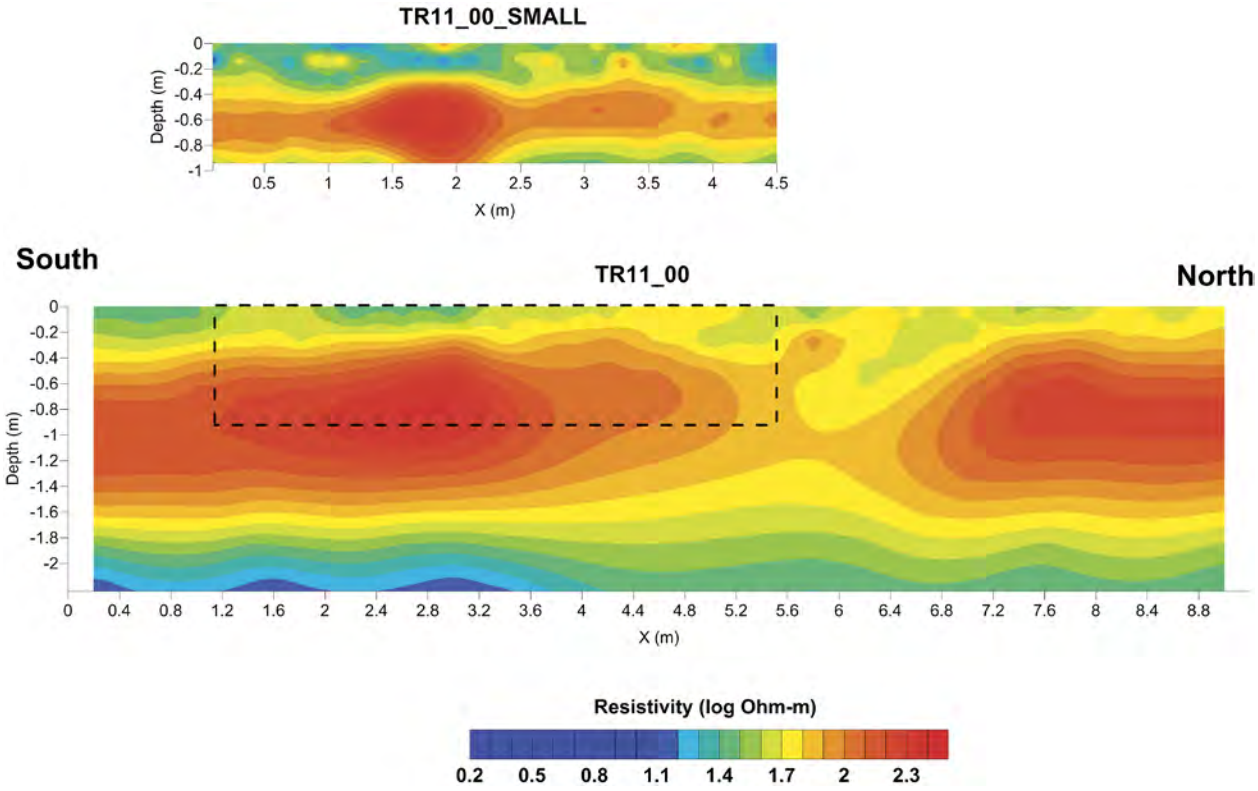

Figure 25. Result of inversion of the resistivity data of the tomographies with 0.2 m electrode spacing (TR11_00_SMALL) and 0.4 m spacing (TR11_00) carried out along the same line. The location of the closely spaced tomography TR11_00_SMALL with respect to TR11_00 is marked by dashed lines.
G. N. Tsokas, P. I. Tsourlos, A. Stampolidis, G. Vargemezis

OVERVIEW OF ARCHAEOLOGICAL RESULTS, 2004–2008

It is not the goal of the present article to provide a detailed comparison of each geophysical anomaly with the size and depth of the architectural features exposed by excavation. Such comparison requires detailed technical analyses and model studies, and is still in progress. Some preliminary observations can be made, but our most important conclusion at present is that geophysical surveys at Mitrou have been an extremely valuable aid to archaeological excavation, enabling us to maximize the efficiency of our activities and reach our goals within the time period allowed by Greek law. Areas containing suggestive geophysical anomalies were targeted for excavation, and these have indeed yielded rich results, making our excavation time very effective. Three-dimensional tomography surveys informed us about the configuration and depth of buried architectural features, allowing accurate planning of their excavation. Geophysical mapping also made it possible to extrapolate our excavation results to a site-wide context, and to formulate much broader interpretations than would have been possible on the basis of excavation and surface survey alone.

In the absence of any ancient architectural features on the present surface of the islet of Mitrou, we decided to explore the northeast and northwest excavation sectors because geophysical mapping indicated that they contained promising buried structures, and they were located in land plots that were of reasonable size to be expropriated, as required by Greek law. In addition, we dug an exploratory trench (LR770; see Fig. 2) in the east-central area, where the resistivity survey hinted at the presence of a third large structure. Our 2004–2008 excavations primarily targeted Late Bronze Age and Early Iron Age levels, and our finds have yielded important new information about two crucial periods of transition in Greek prehistory: the formative period of Mycenaean palatial society, including the rise of a political elite in the early part of the LH period, and the disintegration of this urban, state-level society and its reversion to a simple village-level society at the end of the LH period and in the Early Iron Age.

Our fieldwork has made Mitrou a key site for understanding some of the processes and dynamics that led to the rise of complex society in the Mycenaean era and the development of an archaeologically visible political elite. Until now the study of this period had been hampered by a bias in the data set, since most evidence for an emerging elite came from mortuary contexts—the most famous being the shaft graves at Mycenae. Settlements of this period in southern and central Greece were either poorly preserved or not well studied. Few buildings could plausibly be attributed to these elites, and none had been securely dated as early as the LH I phase.[38] At Mitrou

38. Rutter 2001, p. 146; Shelmerdine 2001, pp. 350–351. Before our discovery of Building D, the earliest securely datable monumental buildings were an incompletely excavated LH II structure at Kakovatos in Elis, and Menelaion Mansion 1 at Sparta, dated to LH IIB. Building F at Krisa in Phokis, said by Shelmerdine to date to LH I, is dated to LH IIIA1 and LH IIIB by Darque (2005, p. 435 and plans 126, 127; Darcque uses the name "Chrysso" instead of "Krisa"). The only monumental structure that may date as early as Building D at Mitrou is a large building with cut stone orthostates and 1-m-thick walls identified by Michael Nelson below the later Mycenaean palace at Pylos and tentatively dated by him to the LH II phase; however, that structure was largely destroyed by the LH IIIA palace (Nelson 2001, pp. 17, 117–125, 181–187, and pers. comm.). Van de Moortel is most grateful to Dr. Nelson for sharing his unpublished dissertation, and discussing the orthostate building at Pylos with her.

Figure 26. The east part of Building D's funerary enclosure seen from the south in 2008. Wall 104 is in the foreground, center, and wall 39 just beyond it at right, running north. Photo R. Vykukal

we found not only a settlement but also two architectural complexes with elite characteristics datable to the formative period, beginning in LH I. In addition, we recovered mortuary evidence for the rise of a political elite. Both the settlement and the elite centers exhibit multiple architectural phases and continue through the LH IIIA2 Early phase, when elsewhere Mycenaean palaces are established. Thus our finds allow for a detailed study of the development of political complexity at Mitrou.

Guided by the geophysical results, we uncovered in the northeast excavation sector an architectural complex of the formative period that we labeled Building D (Figs. 5a, 5b, 6), and 40 m to the northwest we excavated parts of what seems to be another architectural complex of the same period, which we call Building H (Fig. 14). The monumental architecture of Building D signals its elite status (Fig. 26), but excavation thus far has yielded little evidence regarding its function other than its funerary use (see below). In contrast, Building H contained much information about activities that took place there, such as the storage and preparation of cereals (room 1, in trench LE795), the slaughter and consumption of animals (trench LE792), fine dining and drinking (trenches LF790 and LE793), production of stone tools (trench LD791), and pottery mending (room 2, in trench LE793). The fact that these activities are complementary and none are repeated in the eight trenches excavated over an area of more than 20 × 30 m is a good indication that we are indeed dealing with a single architectural complex and not with an assortment of individual households.

The elite status of this putative complex is supported by the exquisite quality of its LH I and LH IIB ceramic tableware, and especially by the discovery, in a burned LH I destruction context east of room 2 (trench LE793), of part of a horse bridle made of deer antler decorated with incised curvilinear patterns, which by its shape and decoration can be identified as an import from the Balkans.[39] Such bridle pieces are exceedingly rare in early LH Greece; they have been found together with chariot

39. Van de Moortel and Zahou, forthcoming, fig. 8. The piece was initially identified by E. Kiriatzi, and its identification confirmed by S. Andreou and J. Maran. Van de Moortel is very grateful to Professor Maran for discussing its importance with her and providing bibliographical references.

equipment decorated with similar motifs in a few elite contexts such as Shaft Graves III, IV, and V at Mycenae, and tholos tomb A at Kakovatos. These finds are thought to reflect an elite exchange network that brought chariot technology from the Balkans to Greece.[40] Given their location along a major route from northern to southern Greece, Mitrou's elite would have been well positioned to take part in this network and adopt horse-driven chariots for elite warfare and display.

We also found evidence in Building H for an economic activity that may have been exploited by Mitrou's elite to bolster its power. Two concentrations of crushed *murex* shells (trench LE792) testify to the manufacture of purple dye in both the LH I and LH II phases. With this discovery Mitrou joins a growing group of Bronze Age sites in the Aegean where purple dye production has been identified. Given the great social prestige the color purple enjoyed in the Near East, it is possible that also in the Aegean the manufacture of purple dye was related to elite consumption and was an important item in the export trade, perhaps used in the elite's acquisition of copper and tin.[41] The evidence of food preparation and luxurious drinking and dining in Building H may represent feasting activity, but more study is needed to confirm this. The importance of feasting in the establishment and support of elite power during the formative and fully palatial periods on the Greek mainland has been much discussed in the scholarly literature.[42]

In addition to using horse-drawn chariots and perhaps wearing purple garments, Mitrou's elite projected its power through impressive architecture, the development of urban planning, and funeral display. Building D is the most imposing structure uncovered at Mitrou. The size of this architectural complex is not known, because it extends beyond our excavation territory to the south and east and its plan is not readily discernible in the resistivity map (Fig. 4). The development of the complex included three architectural phases. In the first phase, dated to the LH I period, most walls were rather thin, but wall 104 already at this time stood out by its greater thickness (ca. 0.70 m) and its unusually large fieldstones roughly cut to a rectangular shape (Fig. 26). During Building D's second and third architectural phases, dated to LH I and LH IIB respectively, a monumental rectangular funerary enclosure was constructed in its northwest corner in conjunction with the installation of elite tomb 73 (see below). This enclosure measured 13.5 × 8.25 m and had unusually thick wall socles, 0.75 m in its LH I phase and 1.00–1.20 m in its LH IIB phase, constructed again of large, roughly cut rectangular fieldstones (Figs. 5a, 5b, 6, 24, 26–28). These walls obviously were meant to impress viewers, and they lend the structure a monumental character. Not only are they much thicker than those of any other contemporary structure excavated at Mitrou or at any contemporary site on the Greek mainland, but their socles were built with the largest stones seen at any structure at the site (Figs. 24, 26–28).[43] Because of its thick walls, this enclosure was clearly visible in the resistivity map (Fig. 4).

The only structure revealed by geophysical survey that approaches Building D in size and in the thickness of its walls is the long rectangular building of grid squares R22–24, located some 50 to 60 m south of Building D (Fig. 11). Our excavation in trench LR770 showed that it, too, belongs to the formative period, its latest architectural phase dating to the LH IIB

Figure 27 ***(opposite, top)*****. The northeast corner of Building D's funerary enclosure excavated in 2005–2007, seen from the east, showing the exterior facade of east wall 39 of Building D and the irregular top of wall 63 running perpendicular to it (foreground right). The full height of wall 39 is visible in the excavated vertical strip left of the center of the image.** Photo S. Vitale

Figure 28 ***(opposite, bottom)*****. State plan of trench LP784 at the end of the 2006 excavation season, showing the northeast corner of Building D's funerary enclosure, and wall 63 branching off in an east-southeast direction.** G. Bianco

40. Penner 1998, pp. 120–123, pls. 38, 40–42, 46, 54. Whereas Penner believed that these bridle and chariot pieces came into Greece with invaders from the north, David (2007) proposes the more plausible interpretation that they were introduced through elite exchange.

41. Burke 1999. Purple-dye manufacture at Mitrou was identified by Rena Veropoulidou.

42. E.g., Halstead and Barrett 2004; Wright 2004.

43. For a list of wall thicknesses of LH buildings, see Darcque 2005, pp. 139–143 (LH I buildings nos. 6, 7, 27, 64, 122, 138, 145, 146, and possibly 150 and 154; LH II buildings nos. 67, 100, 115, 123, 132–137, 149).

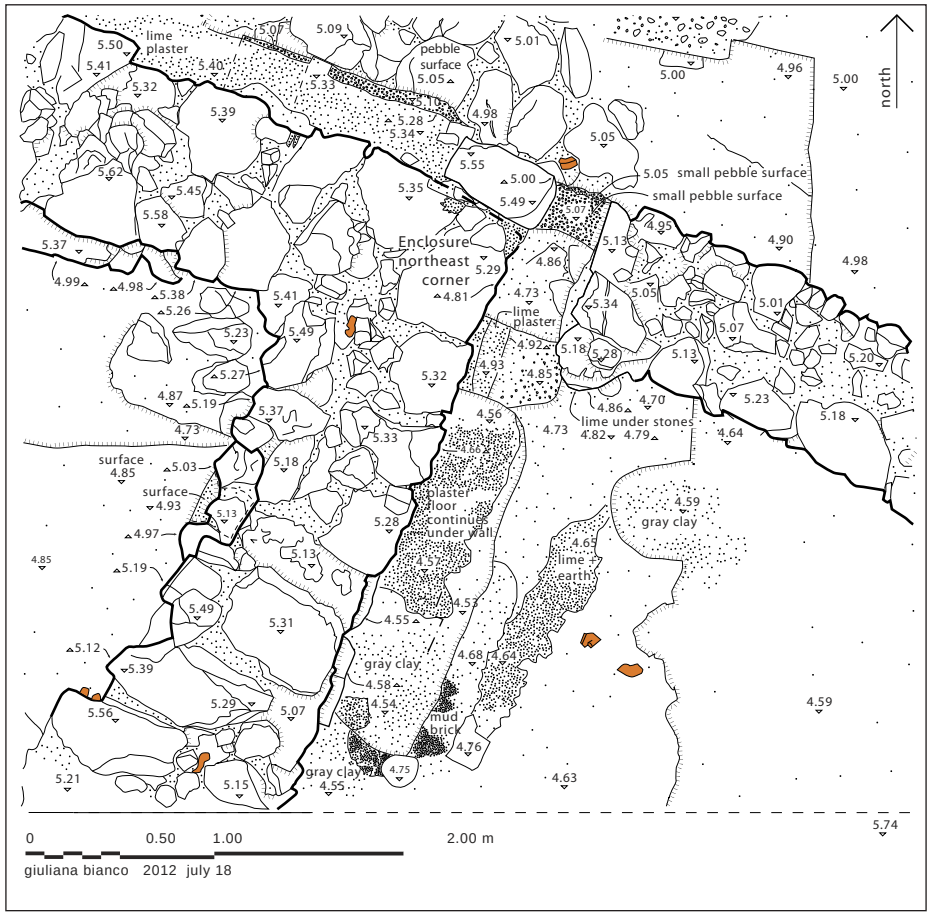
north
lime plaster
pebble surface
small pebble surface
Enclosure northeast corner
lime plaster
lime under stones
surface
plaster floor continues under wall
gray clay
lime + earth
mud brick
gray clay
gray clay
0
0.50
1.00
2.00 m
giuliana bianco 2012 july 18

period. However, its walls are only 0.70–0.80 m thick—much thinner than the maximum thickness of Building D's funerary enclosure walls of the same date—and they are built with much smaller stones (Figs. 8–10). Since the greatest depth reached by geophysical mapping (1.00–1.50 m) encompasses LH and Early Iron Age remains at Mitrou, we may conclude that, on present evidence, Building D's funerary enclosure is more impressive in terms of its size and wall thickness than any other structure of these periods at the site.

Contemporary with the initial construction of Buildings D and H, major changes took place in the layout of the settlement and in burial practices, and the emerging elite at Mitrou is likely to have been involved in both. During the LH I phase, the character of Mitrou's settlement changed from rural to urban. Geophysical mapping indicates that the islet is covered with a dense pattern of buried long orthogonal roads aligned in NNE– SSW and WNW–ESE directions (Fig. 11). Our excavation of parts of four roads as well as our documentation of the east sea scarp of the islet revealed that these roads date to the formative period and were developed in conjunction with elite complexes D and H. Three carefully pebbled streets dating to the LH I phase have been uncovered bordering Building D to the north and west, and Building H to the south. Of road 3 south of Building H only a small part has been exposed, and we do not know its width. Roads 1 and 2 flanking Building D are 3 m wide and meet at right angles (Figs. 5a, 5b, 6, 12). Excavation and geophysical surveys showed that rectilinear structures fronted directly onto these streets on both sides, lending the settlement an urban character. Road 1 west of Building D appears as a broad black band in the electrical resistivity map because it consists of a dense succession of 13 pebbled surfaces topped by fallen wall blocks and a later cobble-and-gravel road (Figs. 4, 7). In the resistivity map the black band of road 1 continues in a straight line for about 80 m north–northeast until it reaches the northeast corner of the islet (Figs. 11, 12). In contrast, road 2 running north of Building D had only one layer of pebbles and for this reason its surface does not show up in the resistivity map. Instead one can trace its outline by the walls of rectilinear structures bordering it to the north and south in grid squares R11 and R13 as well as by a linear depression in the modern surface. These features indicate that road 2 runs in a straight line to the east-southeast for about 60 m until it appears in the eastern sea scarp (trenches LY780, LY781) as a roughly 3-m-wide strip of multiple layers of pebbles.[44] It is unknown how much of this road has been lost to the encroaching sea. These long and wide straight roads at Mitrou are very impressive and unequaled on the Greek mainland during the entire formative period. The only road that surpasses them in size is the 4-m-wide and 90-m-long road of LH IIIA–B date uncovered at Dimini.[45]

The fourth road at Mitrou was excavated to the south of the long rectangular structure in trench LR770 (geophysical grid square R23). Road 4 is a 2-m-wide pebble-and-dirt road running likewise in a WNW–ESE direction, bordered by rectilinear walls on both sides (Figs. 8–10, 12). Its latest surface was laid in the LH IIB phase. Excavation in this trench did not progress deeply enough to establish the road's initial construction date. Running parallel to road 2, some 60 m to the north, and at right angles

44. The relationship of the linear depression at the modern surface and the strip of pebbles in the east sea scarp to the street north of Building D was first noticed by field director Kerill O'Neill.

45. Adrimi-Sismani 2007, pp. 161–162, fig. 15:2.

to road 1, road 4 obviously belongs to the same orthogonal network. Its narrower width and rougher construction is suggestive of a different status, inferior to the carefully paved broad pebbled streets near the settlement's elite complexes, Buildings D and H. The location and orientation of those four excavated roads of the formative period and the structures flanking them correspond exactly to the alignments seen in the geophysical map (Fig. 11). Thus it is reasonable to assume that the long linear alignments revealed by our geophysical surveys over the entire islet represent orthogonal roads belonging to the newly laid out urban settlement of the formative period at Mitrou. These new roads flanked by rectilinear buildings not only gave the settlement an urban character, but they also must have functioned as important venues for elite display, since all were wide enough to accommodate chariots. Road 1 in addition appears to have played a role in elite funerary display.

It is clear from our findings that the emerging elite at Mitrou manipulated the funerary realm in its projection, and perhaps legitimization, of power. The electrical resistivity map (Fig. 11) shows that road 1 runs from Building D to the northeast corner of the islet, where we excavated a grave plot of the formative period containing a large cist grave (no. 51) measuring 1.80 × 1.50 × 0.90 m as well as six densely packed, smaller cist graves with NNE–SSW and ENE–WSW orientations, similar to the roads of the settlement (trench LR797: Figs. 2, 29, 30). One of the smaller graves (no. 50) has been dated by its content to LH I; the others were found robbed of their grave goods, but because of their close proximity are likely to date to roughly the same period.[46] Built with a few large, roughly cut slabs, grave 51 is a monumentalized version of the cist tomb and therefore can be interpreted as an elite grave. Its location appears to have been carefully planned with the intent of maximizing its visibility and dramatic effect: linked to Building D by road 1, the gravesite lay near the highest point of the islet, overlooking the sea.

Still within the LH I phase, an even larger elite grave was constructed inside the northwest part of Building D itself (Fig. 6). A large rectangular built chamber tomb (no. 73) with a burial chamber of ca. 5.00 × 2.00 × 1.20 m was dug through the first floor of Building D and the underlying remains. The chamber was lined with mudbrick walls covered on the interior by large well-finished sandstone orthostates (Fig. 5b). It was enclosed by the monumental rectangular funerary enclosure constructed with 0.75-m-thick walls discussed above. Such a large, well-built tomb set within a high-status building complex represents a major escalation in funerary expenditure and display on the part of the elite. Not only did the tomb chamber alone have a volume almost five times larger than that of the large cist grave 51 in the northeast section of the islet, it was also much more labor-intensive and impressive. In its first phase it was entered from the south side, and its dromos made a 90-degree angle to the west, ending in a porch fronting onto road 1. Grave 73 had been robbed in antiquity, but still contained small fragments of human bones as well as pieces of one or more boar's tusk helmets, arrowheads, LH I pottery, an amber bead, and small gold and silver nails that may have belonged to a wooden chest. In the LH IIB phase, the tomb chamber was extended 2 m to the south, reaching a length of 7.00 m;

46. Cist grave 50 contained a bichrome amphoriskos datable to LH I. The latest pottery fragments below the other graves indicate that they date to MH/LH I or later.

Figure 29. Balloon image of grave plot in trench LR797, in the north-east corner of the islet, at the end of the 2008 excavation season. Photo K. Xenikakis

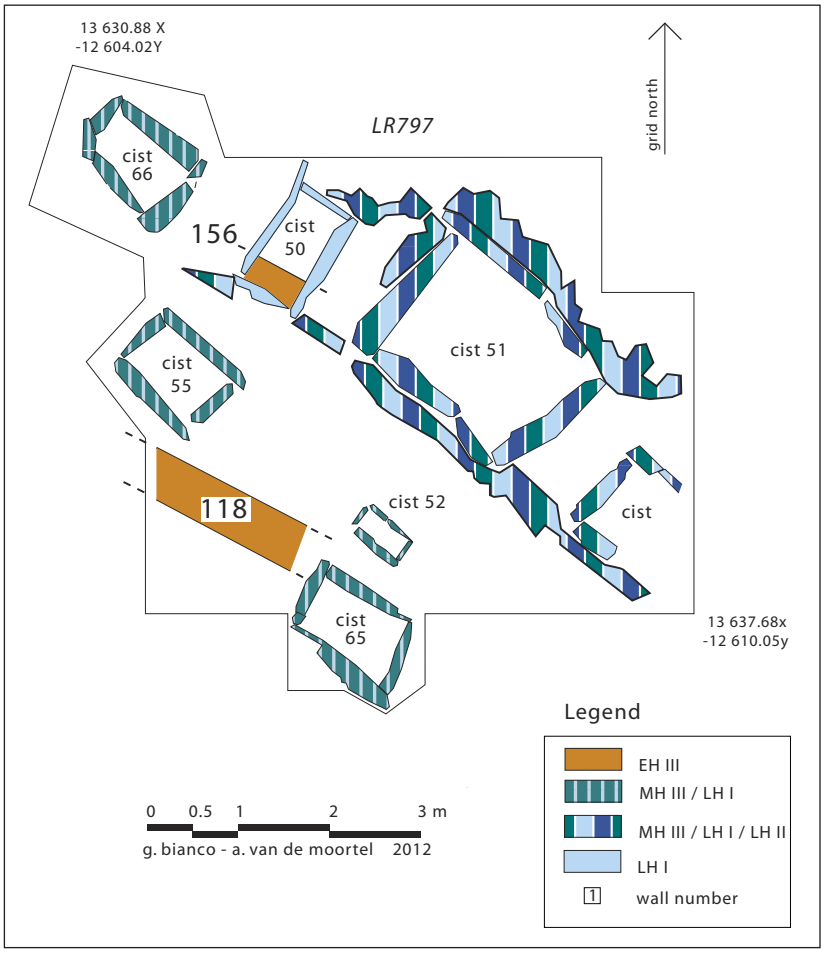

Figure 30. Site plan of trench LR797 in 2008. G. Bianco and A. Van de Moortel

it was now entered from the west. The funerary enclosure was given more substantial walls reaching 1.00 to 1.20 m in thickness. The outlines of the enlarged grave 73 and its funerary enclosure are visible in the 2003 electrical resistivity map (Fig. 4). The remains of this phase had been robbed as well, but again human bone fragments and pieces of a boar's tusk helmet can be associated with it, together with an arrowhead, various pieces of gold and bronze jewelry, a rock-crystal disk, an amber or carnelian bead, and LH IIB as well as LH IIIA1 pottery.

In addition to the construction of elite graves, we see a change in burial practices in Mitrou's settlement early in the formative period. During the MH period and early in the LH I phase, funerary and settlement use alternated in the same areas, the dead being buried in cist graves set in the ruins of abandoned buildings, which at a later date were again covered by buildings. This practice stopped sometime in the LH I phase. The plot of cist graves exposed in trench LR797 in the northeast corner of the islet had been set within the remains of earlier buildings, but it was never built over, and neither were the LH I cist graves uncovered in trench LX784 on the eastern sea scarp of the islet, just north of road 2 (Figs. 2, 13, 29, 30). In addition, it seems that most of the area east of road 1 and north of road 2 was likewise abandoned by settlement during the LH I phase and reserved for funerary usage. This abandonment is suggested by the absence of built structures in the top 0.75 m of grid squares R4 and R13 just west of trench LX784, as revealed by our 2003 electrical resistivity tomography (see above), as well as by the relative scarcity of walls visible in grid squares R5 and R6 of the geophysical map (Fig. 11). Moreover, our surface survey showed that the entire area contains an unusually low proportion of LH pottery. The lack of LH settlement occupation in this area is also indicated by the presence of a MH building close to the modern surface in the adjacent eastern sea scarp.[47] The changes in burial practices at Mitrou fit into a larger trend observed by Joseph Maran at sites from the southern Peloponnese to Thessaly, and they support Maran's hypothesis that the trend signals the rise to power of new elites, who were now in a position to dictate a profound reorganization of their settlements.[48]

The well-organized and obviously planned settlement and funerary areas at Mitrou, which appeared at roughly the same time as the elite centers in the LH I phase, represent a breakthrough in our understanding of the nascent elite on the Greek mainland. It is our first evidence for such a high degree of spatial organization in a settlement of the formative period, and it indicates that the emerging political leadership was well versed in the organization and management of an urban settlement. This level of organization is quite different from that of rural settlements of MH Greece, such as Argos, Malthi, or Asine.[49] It remains to be seen how far this settlement layout was influenced by that of southern Aegean urban settlements such as Ayia Irini on Kea and Phylakopi on Melos, or perhaps Kolonna on Aegina.

Early in the 14th century B.C., the settlement of Mitrou suffered widespread destruction, leading to the deposition of substantial amounts of LH IIIA2 Early pottery in several areas around Building D.[50] Two of these deposits were found west of Building D and may both belong to Building F,

47. This MH structure was documented in archaeological grid squares LX787–LW788, at the northern end of the eastern sea scarp, some 15 m north of trench LX784 (Van de Moortel and Zahou 2011, p. 297, fig. 4).

48. Maran 1995.

49. Cf. Nordquist 1987, pp. 26–29.

50. Van de Moortel and Zahou 2003–2004, p. 41, fig. 5; Van de Moortel 2007, p. 248; Vitale 2008. It is not yet clear what happened in the area of the putative northwest complex, as it suffered substantial erosion of its early LH III levels.

a structure of which only small parts have been uncovered.[51] The pottery in these deposits shows strong Mycenaean characteristics and juvenile pig remains are also present, indicating that already before the destruction Mitrou's elite had adopted Mycenaean cultural practices of ritual eating and drinking.[52] The nature of occupation during the palatial period following the site's destruction is not well understood. Significant amounts of LH IIIA2 Middle–LH IIIB pottery recovered from the site testify to continuity of occupation, but the excavated areas appear to have been largely abandoned.[53] Few architectural remains can be dated to this period, and Building F, neighboring Building D to the west, was only partially reused. The discovery of three fragmentary terracotta roof tiles in association with high-quality LH IIIB2 pottery in a large dump found in the ruins of Building D just east of the funerary enclosure suggests that an administrative building existed at Mitrou during the palatial period.[54] No such structure, however, is apparent on the geophysical survey maps.

After the demise of the Mycenaean palaces, ca. 1200 B.C., much of the urban settlement in the northeast excavation sector at Mitrou was rebuilt, and in LH IIIC Middle a new structure labeled Building B was set on top of the ruins of Building D (Fig. 6).[55] Building B's location might signify that it was intended as Building D's successor. However, in spite of the recovery of a few disturbed earthen floors, no floor deposits can be associated with this structure, and thus we do not know what activities it housed. After Building B went out of use, the small rectangular structure C was built over its northwest corner during the LH IIIC Late phase. Building C's architecture and a floor deposit of 22–26 miniature vases accompanied by a cooking pot with piglet bones indicate that it was not an ordinary domestic structure. It may have been a ritual structure with funerary connotations, purposely buried at an early moment in the LH IIIC Late phase.[56]

In contrast to many other settlements on the Greek mainland, Mitrou apparently was never abandoned during the transition from the Bronze Age to the Iron Age, and thus it is an excellent site at which to study how the urban communities of the Mycenaean period were replaced by the simple villages of the Early Iron Age. This transformation happened at Mitrou in the LH IIIC Late phase, before the end of the Bronze Age. At this time, intramural cist graves were reintroduced at the site, where they were embedded in the ruins of the Bronze Age settlement. This practice continued throughout the PG period (Fig. 6). A poorly preserved small apsidal structure, Building J, was built over the north room of Building B; part of Building F was rebuilt with an exterior courtyard; and south of Building B a new structure, Building G, was constructed also with an exterior courtyard.

51. The excavation of Building F has been temporarily halted because of a land dispute.

52. Vitale 2008.

53. Van de Moortel 2007, p. 249. For the ceramic definition of the LH IIIA2 Early, Middle, and Late subphases at Mitrou, see Vitale 2011.

54. Vitale, forthcoming; Van de Moortel and Zahou, forthcoming.

55. For a more detailed description of Mitrou's LH IIIC settlement, see Van de Moortel 2009. LH IIIC pottery dates have been provided by B. Lis; the LH IIIC Middle date of Building B was determined in 2011.

56. Rutter 2007, pp. 295–296; Lis 2009, pp. 209–210; Van de Moortel 2009, pp. 362–364.

The rubble walls of Building G's courtyard are only 0.20–0.40 m wide and do not show up in the electrical resistance map (cf. Figs. 4 and 5a, 5b). The appearance of exterior courtyards as well as the flimsy nature and crooked outline of Building G represent marked shifts from the earlier urban settlement with its rectilinear buildings lining straight roads. These features are reflective of the rural character of the new settlement. The reasons for these changes are still under investigation.

Early in the Iron Age, toward the end of the Early PG phase or beginning of the Middle PG phase, apsidal Building A was constructed inside the southern part of Building B (Figs. 5a, 6). Building A is one of only 10 apsidal structures known from the Aegean during the PG period, and one of four with substantial floor deposits.[57] Its study is expected to provide valuable new insights into the function of this building type in Early Iron Age society. The quality of Building A's architecture and its substantial size (exterior width = 6.30–6.90 m) as well as the finds within it would make it a good candidate for an Early Iron Age leader's dwelling according to the criteria set out by Mazarakis Ainian.[58] Geophysical mapping and surface surveys again allow us to place excavation finds into a site-wide context. A recent study by Štěpán Rückl of Early Iron Age pottery from our excavation as well as from the 1988–1989 CHELP and 2004–2008 Mitrou surface surveys identified five areas of concentration of Early Iron Age material in the central part of the islet. These areas correspond to places where buried curved walls have been detected by geophysical mapping (Figs. 4, 11: geophysical squares G73 and GR34; R9; R10; R11–R14; and R18–R19 with R23). Rückl's findings led him to conclude that the Early Iron Age settlement at Mitrou consisted of five clusters of curvilinear buildings, each with their own grave plots.[59] More study and excavation are needed to determine whether this settlement was largely egalitarian in character, as Rückl proposes, or whether it had a more hierarchical structure and Building A was indeed the dwelling of its leading household. If its preeminence could be demonstrated, Building A's location inside Building B would provide a unique example of spatial and functional continuity between the final phases of the Bronze Age and the Early Iron Age in the Aegean.

By the Late PG phase, Building A had gone out of use and its apsidal area was turned into an exterior courtyard for a new structure, Building E (Figs. 5a, 6). This rectangular building was set into the southeast part of Building A, effectively destroying the walls of the earlier structure. Building E's walls, 0.60 m thick, were situated at a very shallow depth within the modern plow zone and hence were much disturbed. For reasons not well understood, its southern wall (wall 43) is clearly visible as a black line in the electrical resistivity map, whereas the two parts of its west wall (wall 2) are not visible, even though they have a similar thickness and lie at a shallow depth below the modern surface (cf. Figs. 4, 6, 7). No floor or finds were identified within Building E to inform us about its use. In the exterior courtyard over former Building A, however, we uncovered a small stone platform with crushed *murex* shells adjacent to the west facade of wall 2, as well as two saddle querns, three hearths, and cooking-pot fragments, indicating that purple-dye manufacture was again taking place at Mitrou.[60]

57. Van de Moortel and Zahou 2003–2004, pp. 44–46. For a detailed discussion of Early Iron Age buildings and their social context, see Mazarakis Ainian 1997.

58. Mazarakis Ainian 1997, pp. 271–276.

59. Rückl 2008, pp. 33–38.

60. *Murex*-dye production was again identified by Rena Veropoulidou.

CONCLUSIONS

This preliminary overview of geophysical and archaeological research at Mitrou and its results illustrates the advantages of a close cooperation between geophysicists and archaeologists during all phases of excavation. Geophysics is especially useful at sites such as Mitrou, where no ancient architectural remains are visible on the modern surface. As budget and time constraints did not allow us much opportunity for exploration through excavation, electrical resistance mapping and magnetic gradiometry came to the rescue, revealing optimal areas for excavation and guiding us to relatively quick success. In both the northeast and northwest areas of the islet, geophysical surveys revealed outlines of what looked like buried large apsidal or rectangular structures. Subsequent excavations in these areas indeed uncovered important buildings as well as parts of the adjacent settlement, which are already providing significant new information about crucial phases of sociopolitical change in Greek prehistory.

In addition, resistivity tomographies revealed the three-dimensional shape of ancient structures at specific locations, giving us a fairly precise image of what we would find. The configuration and depth of the northeast corner of Building D's funerary enclosure were indicated by resistivity tomography and confirmed by excavation (Figs. 22–24, 27, 28). This shows that tomography is sensitive enough to predict the shape, size, and depth of buried structures and can be used as a reliable tool in planning their excavation. Geophysical mapping methods furthermore provided images of a well-organized LH urban complex covering the entire islet, as well as clusters of curvilinear structures presumably of Early Iron Age date, helping us to place our excavation and surface survey results in a site-wide context. A final advantage of geophysical prospection is that the whole operation is nondestructive.

Along with these successes, some limitations of the employed geophysical methods have become apparent as well, and it is clear from our work that archaeological excavation remains indispensable for an accurate interpretation of buried structures. The three-dimensional tomographies were unable to distinguish different archaeological strata because of the close succession of these strata and the spatial overlap of buildings of different periods at the same elevations. Only archaeological excavation could disentangle these buildings. Likewise, in the northwest excavation sector both electrical resistivity mapping and magnetic gradiometry suggested the presence of a very large building. Subsequent excavation of some of its walls, however, makes it seem more likely that Building H is an architectural complex composed of smaller structures. Furthermore, in squares R22, R23, and R24 in the east-central part of the islet, the resistivity survey suggested the presence of a double row of large rooms running WNW–ESE. Excavation in trench LR770 showed, however, that the southernmost row of rooms does not exist but is in fact a road (Figs. 8–12). In addition, some excavated walls were not visible on the geophysical map, even though they were located at shallow depths. The reasons for their invisibility are currently being investigated. For now it is important to note that the absence of geophysical anomalies does not necessarily mean a lack of buildings.

Finally, the two long, deep tomographies carried out across the length and breadth of the islet did not clarify entirely the geological setting of the subsurface. Geological study including one or more core drillings is needed to calibrate our geophysical findings so that the conclusions can be extrapolated over the whole length of the tomographies.

Given the large amount of fieldwork and processing required to carry out electrical resistivity tomographies, and the limited financial means normally available for geophysical survey in archaeology, tomography should be considered a supplement to the standard two-dimensional mapping modes of electrical resistivity and magnetometry. In practice, tomographies can be performed only in areas of particular archaeological interest pinpointed by geophysical mapping, but they provide archaeologists with a very useful three-dimensional "sneak preview" into the subsurface.

In spite of its limitations, geophysical survey made an invaluable contribution to our exploration of Mitrou. It was an indispensable tool for zeroing in on the most interesting areas and planning their excavation, and it provided valuable complementary data that enabled us to interpret the excavated areas in a site-wide context. By integrating geophysical survey with archaeological excavation and total-site surface survey we have obtained a much fuller picture of the prehistoric occupation of the islet than would have been possible through excavation alone.

ACKNOWLEDGMENTS

We would like to thank Nina Kyparissi-Apostolika and Maria Papakonstantinou, successive directors of the Ephorate of Lamia, as well as Stephen V. Tracy and Jack L. Davis, successive directors of the American School of Classical Studies at Athens, for their strong support of the Mitrou Archaeological Project. This project was financed by generous contributions from the University of Tennessee (Department of Classics, College of Arts and Sciences, Office of Research, Office of Graduate Studies), the National Endowment for the Humanities (grant no. RZ-50652), the Institute for Aegean Prehistory, the Loeb Classical Library Foundation of Harvard University, the 14th district of the Greek Archaeological Service at Lamia (ID′ EPKA), Colby College, the University of Evansville, and private donors, as well as by one-time contributions from the University of Rhode Island (2005), the University of California at Santa Barbara (2005), the University of Kansas (2007), and Randolph-Macon College (2008). We are very grateful to all for their generosity. We also thank College Year in Athens and Cornell University for administering our field schools. Any views, findings, conclusions, or recommendations expressed in this publication do not necessarily reflect those of the National Endowment for the Humanities.

The preliminary results presented here are the work of the 2004–2008 Mitrou excavation teams, and in particular Giuliana Bianco and Alexandra Costic (architects); Kerill O'Neill, Colby College (field director); Caroline Belz, University of California at Los Angeles (surface survey); Susan Frankenberg and Nicholas Herrmann, University of Tennessee (physical

anthropology); Jeremy B. Rutter, Dartmouth College; Patrick Thomas, University of Evansville; Bartlomiej Lis, Polish Academy of Sciences; Štěpán Rückl, University of Amsterdam; Salvatore Vitale, University of Pisa (pottery analysts); Angeliki Karathanou, University of Thessaloniki (flotation, archaeobotanical remains); Thanos Webb, University of California at Los Angeles (flotation, faunal remains); Rena Veropoulidou, University of Thessaloniki (shells); and Evi Gorogianni, Teresa Hancock Vitale, and Barbara Nielsen Wold (laboratory directors).

REFERENCES

Adrimi-Sismani, V. 2007. "Mycenaean Northern Borders Revisited: New Evidence from Thessaly," in *Rethinking Mycenaean Palaces* 2 (Cotsen Institute of Archaeology Monograph 60), ed. M. L. Galaty and W. A. Parkinson, Los Angeles, pp. 159–177.

Aitken, M. J. 1974. *Physics and Archaeology,* 2nd ed., Oxford.

Aspinall, A., and J. T. Lynam. 1970. "An Induced Polarization Instrument for the Detection of Near Surface Features," *Prospezioni archeologiche* 5, pp. 67–75.

Athanasiou, E., P. I. Tsourlos, G. Vargemezis, C. B. Papazachos, and G. N. Tsokas. 2007. "Nondestructive DC Resistivity Surveying Using Flat-Base Electrodes," *Near Surface Geophysics* 5, pp. 263–272.

Becker, H. 1995. "From Nanotesla to Picotesla: A New Window for Magnetic Prospecting in Archaeology," *Archaeological Prospection* 2, pp. 217–228.

Burke, B. 1999. "Purple and Aegean Textile Trade in the Early Second Millennium B.C.," in *Meletemata: Studies in Aegean Archaeology Presented to Malcolm H. Wiener as He Enters His 65th Year* (*Aegaeum* 20), ed. P. P. Betancourt, V. Karageorghis, R. Laffineur, and W.-D. Niemeier, Liège, pp. 75–82.

Clark, A. J. 1990. *Seeing Beneath the Soil: Prospecting Methods in Archaeology,* London.

Constable, S., R. Parker, and C. Constable. 1987. "Occam's Inversion: A Practical Algorithm for Generating Smooth Models from Electromagnetic Sounding Data," *Geophysics* 52, pp. 289–300.

Dahlin, T. 2001. "The Development of DC Resistivity Imaging Techniques," *Computers and Geosciences* 27, pp. 1019–1029.

Darcque, P. 2005. *L'habitat mycénien: Formes et fonctions de l'espace bâti en Grèce continentale à la fin du II^e^ millénaire avant J.-C.* (*BÉFAR* 319), Athens.

David, W. 2007. "Gold and Bone Artefacts as Evidence of Mutual Contact between the Aegean, the Carpathian Basin, and Southern Germany in the Second Millennium B.C.," in *Between the Aegean and Baltic Seas: Prehistory Across Borders. Proceedings of the International Conference "Bronze and Early Iron Age Interconnections and Contemporary Developments between the Aegean and the Regions of the Balkan Peninsula, Central and North Europe," University of Zagreb, 11–14 April 2005* (*Aegaeum* 27), ed. I. Galanaki, H. Tomas, Y. Galanakis, and R. Laffineur, Liège, pp. 411–420.

Fossey, J. M. 1990. *The Ancient Topography of Opountian Lokris,* Amsterdam.

Green, M. D. 2011. "A Geographical Analysis of the Atalanti Alluvial Plain and Coastline as the Location of a Potential Tourist Site: Bronze through Early Iron Age Mitrou, East-Central Greece," *Applied Geography* 32, pp. 335–349.

Halstead, P., and J. C. Barrett, eds. 2004. *Food, Cuisine, and Society in Prehistoric Greece* (Sheffield Studies in Aegean Archaeology 5), Oxford.

Hope Simpson, R., and O. T. P. K. Dickinson. 1979. *A Gazetteer of Aegean Civilisation in the Bronze Age* 1: *The Mainland and Islands* (*SIMA* 52), Göteborg.

Institute for Geology and Subsurface Research (currently IGME—Institute for Geology and Mineral Exploration). 1965. *Geological Map of Greece, Sheet: Atalanti.*

Kramer-Hajos, M. T. 2008. *Beyond the Palace: Mycenaean East Lokris* (*BAR-IS* 1781), Oxford.

Kramer-Hajos, M. T., and K. O'Neill. 2008. "The Bronze Age Site of Mitrou in East Lokris: Finds from the 1988–1989 Surface Survey," *Hesperia* 77, pp. 163–250.

Linford, N. 2006. "The Application of Geophysical Methods to Archaeological Prospection," *Reports on Progress in Physics* 69, pp. 2205–2257.

Lis, B. 2009. "The Sequence of Late Bronze/Early Iron Age Pottery from Central Greek Settlements: A Fresh Look at Old and New Evidence," in *LH III C Chronology and Synchronisms* 3: *LH III C Late and the Transition to the Early Iron Age. Proceedings of the International Workshop Held at the Austrian Academy of Sciences at Vienna, February 23rd and 24th, 2007* (*DenkschrWien* 384), ed. S. Deger-Jalkotzy and A. E. Bächle, Vienna, pp. 203–233.

Maran, J. 1995. "Structural Changes in the Pattern of Settlement during the Shaft Grave Period on the Greek Mainland," in *Politeia: Society and State in the Aegean Bronze Age. Proceedings of the 5th International Aegean Conference, University of Heidelberg, Archäologisches Institut, 10–13 April 1994* (*Aegaeum* 12), ed. R. Laffineur and W.-D. Niemeier, Liège, pp. 67–72.

Mazarakis Ainian, A. 1997. *From Rulers' Dwellings to Temples: Architecture, Religion, and Society in Early Iron Age Greece (1100–700 B.C.)* (*SIMA* 121), Jonsered.

Meju, M. A. 1994. *Geophysical Data Analysis: Understanding Inverse Problem Theory and Practice* (Course Note Series 6, Society of Exploration Geophysicists), Tulsa.

Nelson, M. C. 2001. "The Architecture of Epano Englianos, Greece" (diss. Univ. of Toronto).

Nordquist, G. C. 1987. *A Middle Helladic Village: Asine in the Argolid* (*Boreas* 12), Uppsala.

Penner, S. 1998. *Schliemanns Schachtgräberrund und der europäische Nordosten: Studien zur Herkunft der frühmykenischen Streitwagenausstattung* (Saarbrücker Beiträge zur Altertumskunde 60), Bonn.

Rückl, Š. 2008. "Spatial Layout of the Protogeometric Settlement at Mitrou, East Lokris (Central Greece): Social Reality of a Greek Village in the 10th Century B.C." (M.A. thesis, Univ. of Sheffield).

Rutter, J. B. 2001. "Review of Aegean Prehistory II: The Prepalatial Bronze Age of the Southern and Central Greek Mainland," in *Aegean Prehistory: A Review* (*AJA* Suppl. 1), ed. T. Cullen, Boston, pp. 95–155.

———. 2007. "How Different Is LH III C Middle at Mitrou? An Initial Comparison with Kalapodi, Kynos, and Lefkandi," in *LH III C Chronology and Synchronisms* 2: *LH III C Middle. Proceedings of the International Workshop Held at the Austrian Academy of Sciences at Vienna, October 29th and 30th, 2004* (Veröffentlichungen der mykenischen Kommmission 28), ed. S. Deger-Jalkotzy and M. Zavadil, Vienna, pp. 287–300.

Scollar, I., B. Weidner, and K. Segeth. 1986. "Display of Archaeological Magnetic Data," *Geophysics* 51, pp. 623–633.

Sharma, P. V. 1997. *Environmental and Engineering Geophysics,* New York.

Shelmerdine, C. W. 2001. "Review of Aegean Prehistory VI: The Palatial Bronze Age of the Southern and Central Greek Mainland," in *Aegean Prehistory: A Review* (*AJA* Suppl. 1), ed. T. Cullen, Boston, pp. 329–381.

Sheriff, R. E. 1981. *Encyclopedic Dictionary of Exploration Geophysics,* Tulsa.

Soter, S., V. Murphy, D. Katsonopoulou, and R. Reeves. 2005. "A Strong Magnetic Anomaly at the Bronze Age Site of Mitrou, Lokris, Greece," in *Ancient Helike and Aigialeia: Archaeological Sites in Geologically Active Regions. Proceedings of the Third International Conference on Ancient Helike and Aigialeia, Organized by the Helike Society and the Municipality of Diakopton, 6–9 October 2000* (Helike 3), ed. D. Katsonopoulou, S. Soter, and I. K. Koukouvelas, Athens, pp. 303–310.

Tsokas, G. N., P. I. Tsourlos, and N. Papadopoulos. 2008. "Electrical Resistivity Tomography: A Flexible Technique in Solving Problems of Archaeological Research," in *Seeing the Unseen: Geophysics and Landscape Archaeology,* ed. S. Campana and S. Piro, Leiden, pp. 83–104.

Tsokas, G. N., P. I. Tsourlos, A. Stampolidis, R. Hamza, N. Diamanti, and M. Tsapanos. 2003. "Γεωφυσική διασκόπιση στη νησίδα Μήτρου." Report submitted to the 14th Ephorate of Prehistoric and Classical Antiquities (Ministry of Culture, Greece). Project 21414, Research Committee, Aristotle University of Thessaloniki.

Tsokas, G. N., P. I. Tsourlos, G. Vargemezis, and M. Novack. 2008. "Non-Destructive Electrical Resistivity Tomography for Indoor Investigation: The Case of Kapnikarea Church in Athens," *Archaeological Prospection* 15, pp. 47–61.

Tsourlos, P. I. 1995. "Modelling Interpretation and Inversion of Multi-electrode Resistivity Survey Data" (diss. Univ. of York).

Tsourlos, P. I., R. D. Ogilvy, and C. Papazachos. 2004. "Borehole-to-Surface ERT Inversion," in *Proceedings of the 10th European Meeting of Environmental and Engineering Geophysics, 6–9 September 2004, Utrecht* (extended abstract), http://www.earthdoc.org/detail.php?pubid=1725 (accessed August 2012).

Tsourlos, P. I., and G. N. Tsokas. 2011. "Non-Destructive Electrical Resistivity Tomography Survey at the South Walls of the Acropolis of Athens," *Archaeological Prospection* 18, pp. 173–186.

Tsourlos, P. I., G. N. Tsokas, N. Papadopoulos, V. Manidaki, M. Ioannidou, and A. Sarris. 2006. "Non-Destructive ERT Survey at the South Wall of Akropolis of Athens, Greece," in *Proceedings of the 12th European Meeting of Environmental and Engineering Geophysics, 4–6 September 2006, Helsinki* (extended abstract), http://www.earthdoc.org/detail.php?pubid=626 (accessed August 2012).

Van de Moortel, A. 2007. "The Site of Mitrou and the North Euboean Gulf in Homeric Times," in *EPOS: Reconsidering Greek Epic and Aegean Bronze Age Archaeology. Proceedings of the 11th International Aegean Conference, Los Angeles, UCLA, The J. Paul Getty Villa, 20–23 April 2006* (*Aegaeum* 28), ed. S. P. Morris and R. Laffineur, Liège, pp. 243–254.

———. 2009. "The Late Helladic IIIC–Protogeometric Transition at Mitrou, East Lokris," in *LH III C Chronology and Synchronisms* 3: *LH III C Late and the Transition to the Early Iron Age. Proceedings of the International Workshop Held at the Austrian Academy of Sciences at Vienna, February 23rd and 24th, 2007* (*DenkschrWien* 384), ed. S. Deger-Jalkotzy and A. E. Bächle, Vienna, pp. 359–372.

Van de Moortel, A., and E. Zahou. 2003–2004. "Excavations at Mitrou, East Lokris," *Aegean Archaeology* 7, pp. 39–48.

———. 2011. "The Bronze Age–Iron Age Transition at Mitrou, in East Lokris: Evidence for Continuity and Discontinuity," in *The "Dark Ages" Revisited. Acts of an International Conference in Memory of William D. E. Coulson, University of Thessaly, Volos, Greece, 14–17 June 2007,* ed. A. Mazarakis Ainian, Volos, pp. 287–303.

———. Forthcoming. "Five Years of Archaeological Excavation at the Bronze Age and Early Iron Age

Site of Mitrou, East Lokris (2004–2008): Preliminary Results," in *3rd Archaeological Meeting of Thessaly and Central Greece, 2006–2008: From Prehistory to the Contemporary Period, Volos, 12–15 March 2009,* ed. A. Mazarakis Ainian and A. Doulgeri-Intzesioglou, Volos.

Vitale, S. 2008. "Ritual Drinking and Eating at Late Helladic IIIA2 Early Mitrou, East Lokris: Evidence for Mycenaean Feasting Activities?" in *Dais: The Aegean Feast. Proceedings of the 12th International Aegean Conference Held at the University of Melbourne, Centre for Classics and Archaeology, 25–29 March 2008* (*Aegaeum* 29), ed. L. A. Hitchcock, R. Laffineur, and J. Crowley, Liège, pp. 229–237.

———. 2011. "Late Helladic IIIA:2 Pottery from Mitrou and Its Implications for the Ceramic Chronology of the Mycenaean Mainland," in *Our Cups Are Full: Pottery and Society in the Aegean Bronze Age. Papers Presented to Jeremy B. Rutter on the Occasion of His 65th Birthday,* ed. W. Gauss, M. Lindblom, R. A. K. Smith, and J. C. Wright, Oxford, pp. 331–344.

———. Forthcoming. "Local Traditions and Mycenaeanization in North-Central Greece: A Preliminary Report on the Late Helladic II to Late Helladic IIIB Pottery from Mitrou, East Lokris, and Its Significance," in *3rd Archaeological Meeting of Thessaly and Central Greece, 2006–2008: From Prehistory to the Contemporary Period, Volos, 12–15 March 2009,* ed. A. Mazarakis Ainian and A. Doulgeri-Intzesioglou, Volos.

Ward, S. H. 1990. "Resistivity and Induced Polarization Methods," in *Geotechnical and Environmental Geophysics* 1: *Review and Tutorial* (Investigations in Geophysics 5), ed. S. H. Ward, Tulsa, pp. 147–189.

Wright, J. C., ed. 2004. *The Mycenaean Feast*, Princeton.

Gregory N. Tsokas

Aristotle University of Thessaloniki
school of geology
department of geophysics
laboratory of exploration geophysics
54124 thessaloniki
greece

gtsokas@geo.auth.gr

Aleydis Van de Moortel

University of Tennessee
department of classics
1101 McClung tower
knoxville, tennessee 37996–0413

avdm@utk.edu

Panayiotis I. Tsourlos

Aristotle University of Thessaloniki
school of geology
department of geophysics
laboratory of exploration geophysics
54124 thessaloniki
greece

tsourlos@geo.auth.gr

Alexandros Stampolidis

Aristotle University of Thessaloniki
school of geology
department of geophysics
laboratory of exploration geophysics
54124 thessaloniki
greece

astamp@geo.auth.gr

George Vargemezis

Aristotle University of Thessaloniki
school of geology
department of geophysics
laboratory of exploration geophysics
54124 thessaloniki
greece

varge@geo.auth.gr

Eleni Zahou

14th Ephorate of Prehistoric and Classical Antiquities
kastro
35100 lamia
greece

zahel_28@hotmail.com